

1 **Methane, ethane, and propane production in Greenland ice**
2 **core samples and a first isotopic characterization of excess**
3 **methane**

4 Michaela, Mühl¹, Jochen Schmitt¹, Barbara Seth¹, James E. Lee², Jon S. Edwards³, Edward J.
5 Brook³, Thomas Blunier⁴, Hubertus Fischer¹

6
7 ¹Climate and Environmental Physics and Oeschger Centre for Climate Change Research, University of Bern,
8 Bern, 3012, Switzerland

9 ²Los Alamos National Laboratory, Earth Systems Observation, Los Alamos, NM 87545, USA

10 ³College of Earth, Ocean, and Atmospheric Sciences, Oregon State University, Corvallis, OR 97331, USA

11 ⁴Centre for Ice and Climate, Niels Bohr Institute, University of Copenhagen, Copenhagen, 2200, Denmark

12
13 *Correspondence to:* Michaela Mühl (michaela.muehl@unibe.ch)

14

15

16

17

18

19

20

21

22

23

24

25

26

27

28

29

30

31

32

33

34

35

Abstract. Air trapped in polar ice provides unique records of the past atmospheric composition ranging from key greenhouse gases such as methane (CH_4) to short-lived trace gases like ethane (C_2H_6) and propane (C_3H_8). Recently, the comparison of CH_4 records obtained using different extraction methods revealed disagreements in the CH_4 concentration for the last glacial in Greenland ice. Elevated methane levels were detected in dust-rich ice core sections measured discretely pointing to a process sensitive to the melt extraction technique. To shed light on the underlying mechanism, we performed targeted experiments and analyzed samples for methane and the short-chain alkanes ethane and propane covering the time interval from 12 to 42 kyears. Here, we report our findings of these elevated alkane concentrations, which scale linearly with the amount of mineral dust within the ice samples. The alkane production happens during the melt extraction step of the classic wet extraction technique and reaches 14 to 91 ppb of CH_4 excess in dusty ice samples. We document for the first time a co-production of excess methane, ethane, and propane, with the observed concentrations for ethane and propane exceeding their past atmospheric background at least by a factor of 10. Independent of the produced amounts, excess alkanes were produced in a fixed molar ratio of approximately 14:2:1, indicating a shared origin. The measured carbon isotopic signature of excess methane is $(-47.0 \pm 2.9) \text{‰}$ and its deuterium isotopic signature is $(-326 \pm 57) \text{‰}$. With the co-production ratios of excess alkanes and the isotopic composition of excess methane we established a fingerprint that allows us to constrain potential formation processes. This fingerprint is not in line with a microbial origin. Moreover, an adsorption-desorption process of thermogenic gas on dust particles transported to Greenland appears not very likely. Instead, the alkane pattern appears to be indicative of abiotic decomposition of organic matter as found in soils and plant leaves.

hat gelöscht: in the samples analyzed

hat gelöscht: Rather

1. Introduction

Atmospheric air entrapped in polar ice represents a unique archive of the past atmospheric composition including the concentration of greenhouse gases like carbon dioxide (CO_2), methane (CH_4), and nitrous oxide (N_2O) but also short-lived trace gases such as ethane (C_2H_6) and propane (C_3H_8). The ongoing anthropogenic increase in the atmospheric concentrations of these gases makes a detailed understanding of their preindustrial variations and biogeochemical cycling of paramount importance, and only polar ice cores are able to provide this information. However, to interpret reconstructions of the atmospheric composition from polar ice cores requires that archived atmospheric trace gases are not altered within the ice itself. Furthermore, the air must be extracted from the ice sample without altering the original composition. Thus,

71 the comparison of ice core records obtained using different extraction techniques and from
72 different ice cores requires careful consideration and interpretation.

73
74 Not all drill sites or specific time intervals are equally suitable to derive pristine atmospheric
75 trace gas records. For example, CO₂ data from Greenland ice are subject to CO₂ in situ
76 production due to impurities in the ice (Anklin et al., 1995; Smith et al., 1997). In situ
77 production is also observed for N₂O, for example, in glacial Antarctic ice core samples
78 characterized by higher dust content (Schilt et al., 2010). In contrast, CH₄ in polar ice cores, in
79 the absence of melt layers, was considered to be not affected by in situ processes. However,
80 more recent results from Greenland ice showing elevated CH₄ concentrations in glacial dust-
81 rich ice (Lee et al., 2020) and high amplitude CH₄ spikes in Holocene ice (Rhodes et al., 2013,
82 2016) question this assumption.

83
84 This becomes especially worrisome as atmospheric methane shows a significant North-South
85 gradient, reflecting the predominance of Northern Hemisphere sources. Ice cores from
86 Greenland and Antarctica have been used to quantify this Inter-Polar Difference (IPD) in past
87 CH₄ concentrations (Chappellaz et al., 1997; Baumgartner et al., 2012; Beck et al., 2018) to
88 derive the relative contribution of Northern and Southern hemispheric sources to the overall
89 CH₄ changes. The Holocene IPD is on the order of several tens of ppb, i.e., one order of
90 magnitude smaller than the past atmospheric CH₄ concentration. Thus, any small CH₄ bias on
91 the order of a few ppb to tens of ppb strongly impacts the conclusions drawn from this IPD,
92 while the influence on the total radiative forcing by such small biases is negligible. In summary,
93 existing results of CH₄ concentrations from Greenland and Antarctic ice cores have to be
94 carefully scrutinized for such effects.

95
96 A first step in this direction has been made in previous work by Lee et al. (2020), for example
97 by comparing CH₄ records derived using different measurement techniques. Past CH₄
98 concentrations ([CH₄]) are retrieved by measurements of Greenland and Antarctic ice cores
99 using traditional discrete and relatively new continuous melt extraction techniques. While
100 discrete ice measurements deliver one single value for each sample, Continuous Flow Analysis
101 (CFA) gradually melts a thin stick of the ice core providing a continuous record for this section.
102 Although in both techniques the ice sample is melted, the CFA technique separates air from the
103 meltwater stream in about 1-2 min providing only a short time for any reaction in the water,
104 while for the discrete technique the contact time is typically 15-30 min. Comparing [CH₄]

hat gelöscht: It is known that n

hat gelöscht: such

hat gelöscht: with the goal

hat gelöscht: has a

hat gelöscht: on

hat gelöscht: c

hat gelöscht: s

112 histories from several Greenland ice cores measured discretely (NGRIP, GISP2, GRIP) with
113 the continuous Greenland NEEM and the continuous Antarctic WAIS records over the last
114 glacial period, higher [CH₄] can be found in the discrete Greenland measurements for specific
115 time intervals (Lee et al., 2020; Fig. 1 therein), where dust concentrations are especially high.

116
117 Looking at the NGRIP methane hydrogen isotope ($\delta\text{D-CH}_4$) record (Bock et al., 2010b), which
118 was also measured with a discrete melt extraction technique (Bock et al., 2010a), it turns out
119 that in the high dust ice sections, the isotopic values are also affected. Several negative $\delta\text{D-CH}_4$
120 excursions with a maximum depletion of 16 ‰ (permil) prior to the onset of Dansgaard-
121 Oeschger (DO) event 8 were identified (Bock et al., 2010b). At the time of that publication
122 there was no straightforward explanation for these $\delta\text{D-CH}_4$ depletions during times of a
123 relatively stable climate. Using ice from Antarctica, much smaller $\delta\text{D-CH}_4$ variations (3–4 ‰)
124 during this interval were found in measurements performed at the University of Bern
125 (unpublished data), again questioning the atmospheric origin of these $\delta\text{D-CH}_4$ depletions prior
126 to the DO onset.

127
128 All these observations in Greenland ice give reason to assume that a hitherto unknown process
129 exists that produces or releases additional methane in some time intervals in Greenland ice
130 cores (from here on referred to as “excess methane” or CH_{4(x)}). This process is related to the
131 extraction technique (only found in records obtained by discrete melt extractions) and has only
132 been observed in glacial Greenland ice with high mineral dust concentrations.

133
134 A first attempt to characterize CH_{4(x)} was made by Lee et al. (2020) who analyzed [CH₄] in
135 discrete ice samples with different impurity composition and concentration from several ice
136 cores (GISP2, NEEM, WAIS, SPICE) using a multiple melt-refreeze technique. They were able
137 to quantify CH_{4(x)} contributions of up to 30–40 ppb for Greenland samples. Sequential melt-
138 refreeze extractions showed that the process leading to CH_{4(x)} is slow and not completed during
139 the first melt-refreeze cycle (i.e., within around 30 min). A set of samples was analyzed with
140 the admixture of a HgCl₂ solution to suppress microbial activity in the meltwater. No difference
141 in the measured [CH₄] was observed between the poisoned samples and replicates without
142 HgCl₂, excluding a microbial CH₄ production after melting. In addition, Lee et al. (2020) used
143 the NGRIP [CH₄] (Baumgartner et al., 2014) and $\delta\text{D-CH}_4$ records (Bock et al., 2010b) to
144 estimate the deuterium isotopic signature of the CH_{4(x)}. Assuming a two-component mixture

hat gelöscht:

hat gelöscht: hydrogen isotopic

hat gelöscht: that could lead to “lighter” $\delta\text{D-CH}_4$ values

hat gelöscht:

hat gelöscht: variations

hat gelöscht: recorded

hat gelöscht: special

hat gelöscht:

153 of atmospheric methane and excess methane, their model led to a best estimate of (-293 ± 31)
154 ‰ for $\delta D-CH_{4(xs)}$.

155

156 A straightforward explanation for $CH_{4(xs)}$ may be that CH_4 is either produced in the meltwater,
157 or it was produced beforehand and only released during the melt extraction. With respect to
158 that, Lee et al. (2020) reviewed several mechanisms that could account for the observed
159 variations in Greenland ice core records. None perfectly matched all their observations but
160 lastly, three of the proposed mechanisms were short-listed by Lee et al. (2020): (1) an
161 adsorption process on dust particles prior to the deposition on the ice sheet; (2) an in situ
162 production in the ice; or (3) an abiotic reaction during melt extraction.

163

164 Here we resume the work by Lee et al. (2020) and shed more light upon the potential formation
165 processes using a targeted and more comprehensive study to quantify $CH_{4(xs)}$. We analyzed
166 specific NGRIP and GRIP ice core samples discretely with two different wet extraction
167 systems. With our $\delta^{13}C-CH_4$ device we are able to measure [methane], [ethane], [propane], and
168 $\delta^{13}C-CH_4$ on a single ice sample in two subsequent extractions. With our second device we add
169 experimental information on $\delta D-CH_4$. In Sect. 2, we provide information on our sampling
170 strategy and measurement techniques. With our new experimental results, presented in Sect. 3,
171 we provide quantitative data for $CH_{4(xs)}$ in NGRIP and GRIP samples and extend our
172 observations to other “excess alkanes” (ethane and propane), which are revealed to be co-
173 produced during the excess CH_4 production. The observed molar ratios between methane,
174 ethane, and propane are evaluated and their relation to the abundance of mineral dust (Ca^{2+})
175 within the ice samples is quantified. A 2nd extraction of the meltwater enables us to estimate
176 the temporal dynamics of excess alkane production. Using a Keeling-plot approach to our
177 isotopic results, we calculate the carbon and deuterium isotopic signature of excess CH_4 ($\delta^{13}C-$
178 $CH_{4(xs)}$ and $\delta D-CH_{4(xs)}$). Based on our new and improved observations, we finally come back
179 to the discussion of the hypotheses proposed by Lee et al. (2020) in Sect. 4 and offer potential
180 mechanisms that could explain the excess alkanes in ice core samples. For readers not interested
181 in all the experimental details, we recommend to jump straight to Sect. 4 to see the discussion.

182

183 2. Ice core samples and measurements

184 2.1 Ice core samples

185

hat gelöscht: evidence

hat gelöscht: disussion

188 Mixing ratios of alkanes (methane, ethane, and propane) and the stable carbon ($\delta^{13}\text{C}-\text{CH}_4$) and
189 hydrogen ($\delta\text{D}-\text{CH}_4$) isotope ratios of methane were measured on ice core samples from the
190 North Greenland Ice Core Project (NGRIP) ice core. For this study, 19 NGRIP ice core samples
191 were measured for $\delta^{13}\text{C}-\text{CH}_4$ and alkane concentrations and nine NGRIP ice samples for $\delta\text{D}-$
192 CH_4 covering the depth between 1795.84 m and 1933.25 m. The NGRIP samples are from the
193 late glacial Marine Isotope Stages (MIS) 3 and 2 (22.6 to 30.6 kyears BP). These time intervals
194 are characterized by sharp atmospheric CH_4 increases in parallel to rapid warmings, the so-
195 called Dansgaard-Oeschger events, but we mostly sampled intervals with stable CH_4
196 concentrations. From the same time period, we also investigate measurements of 41 NGRIP
197 and 12 GRIP ice core samples which were carried out in 2011 and 2018, respectively, and
198 which have not previously been published. See Fig. 1 for an overview of all analyzed NGRIP
199 and GRIP ice core samples over time.

hat gelöscht: a total of

201 We also included 22 ice core samples from the European Project for Ice Coring in Antarctica
202 (EPICA) ice core from Dome C (MIS 4), which are not affected by a measurable excess CH_4
203 production and which we use as long-term monitoring ice for the system performance and to
204 quantify the blank contribution of the analytical system (see Appendix B).

hat gelöscht: e

205 The late glacial period, which includes the age of most of the measured NGRIP samples, is
206 characterized by an overall high impurity and dust content and low atmospheric methane
207 concentrations. For our analysis, we have selected ice core bags (where for NGRIP and GRIP
208 ice cores, a bag is a 55 cm long ice core section) in which we expect the same atmospheric CH_4
209 concentration but see a high range of mineral dust content (Ca^{2+}). In this way, we can compare
210 neighbouring samples with the same low stadial CH_4 levels due to stable atmospheric
211 concentrations and temporal smoothing by the slow bubble enclosure process but are expected
212 to vary in measured concentrations due to contributions of excess alkanes. Ca^{2+} content across
213 our NGRIP samples ranges from 307 ng/g to 1311 ng/g. This sample selection is critical to
214 quantify the isotope signature of the $\text{CH}_{4(\text{xs})}$ produced using the Keeling-plot approach (Keeling,
215 1958). The underlying assumptions of this mass balance approach are (1) that there is only a
216 two-component mixture (atmospheric methane and excess methane) and (2) that the isotopic
217 ratio of the mixture changes only by a varying input of the second source ($\text{CH}_{4(\text{xs})}$).

hat gelöscht: time

hat gelöscht: that have

hat gelöscht: also

hat gelöscht: isotopic

hat gelöscht:

hat gelöscht: (1)

hat gelöscht: (2)

218
219 To select the samples, we use high-resolution mineral dust records measured using an Abakus
220 laser attenuation device (Klotz, Germany) for particulate dust (Ruth et al., 2003) as well as Ca^{2+}
221 concentrations (Erhardt et al., 2022) as dissolved mineral dust tracer derived from the Bern

Continuous Flow Analysis System (Kaufmann et al., 2008). In principle, particulate dust and the soluble dust tracer Ca^{2+} are strongly correlated. However, depending on acidity of the ice (mainly due to H_2SO_4 and HNO_3), variable amounts of CaCO_3 are converted into soluble CaSO_4 and $\text{Ca}(\text{NO}_3)_2$ leading to a variable Ca^{2+} /dust ratio (Legrand and Delmas, 1988). As an example, Fig. 2 shows the Ca^{2+} and mineral dust concentration of the NGRIP bag 3292 which we used to select the individual samples and the relevant parameters measured for each sample of this bag. The data overview for all other measured NGRIP bags can be found in Appendix A.

hat gelöscht:

hat gelöscht: specific

hat gelöscht: ,

hat gelöscht: the

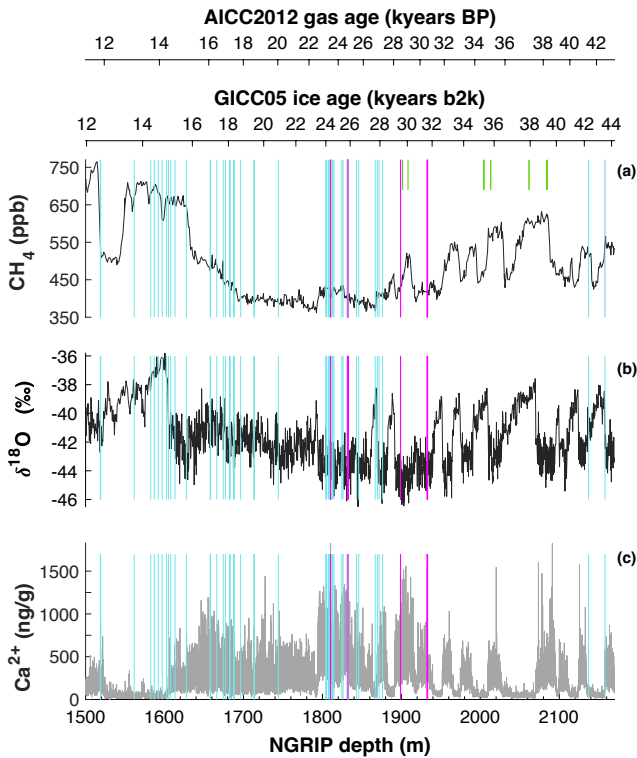


Figure 1: Overview of the analyzed NGRIP and GRIP samples over time. All analyzed NGRIP and GRIP ice core samples are indicated on the NGRIP depth (m) on the bottom axis. To indicate an age for the gas and ice records both the AICC2012 gas age (kyears BP) and the GICC05 ice age (kyears b2k) scale are provided on the upper axes. Note that for the purpose of describing the excess CH_4 production in a certain ice sample the age is not important and we provide all records on depths throughout this manuscript. NGRIP samples measured from the five main bags (3292, 3331 & 3332, 3453, 3515) for the Keeling-plot approach are indicated with vertical lines in pink, NGRIP samples measured in 2011 and individual NGRIP ice core samples measured in 2019-2020 (not included in the Keeling-plot analyses) in turquoise, and GRIP ice core samples measured in 2019-2020 (not included in the Keeling-plot analyses) in green. (a) $[\text{CH}_4]$ record measured by wet extraction from NGRIP samples from Baumgartner et al. (2012, 2014). (b) $\delta^{18}\text{O}$ record from North Greenland Ice Core Project members (2004). (c) Ca^{2+} record from Erhardt et al. (2022).

hat gelöscht: absolute

hat gelöscht: s irrelevant

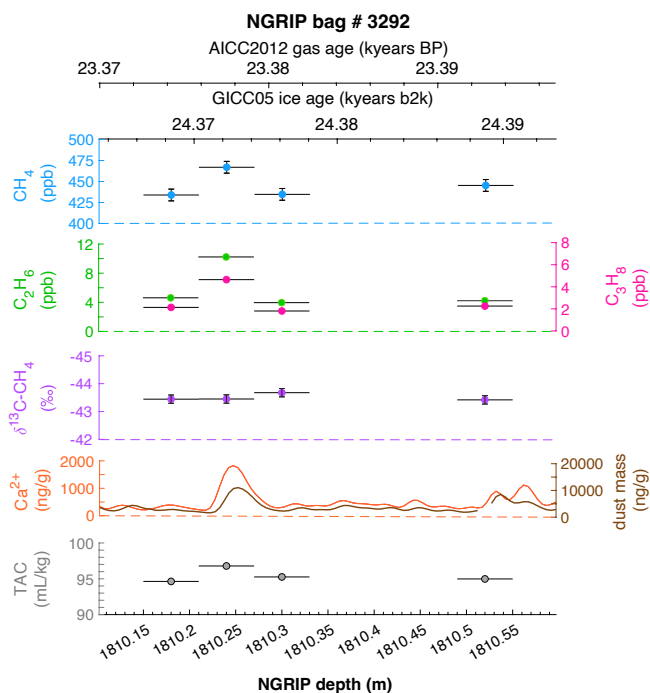


Figure 2: **Detailed data overview for NGRIP bag 3292.** Bag-specific overview of several parameters measured for each sample in this bag at a given depth: methane, ethane, propane, Ca^{2+} , mineral dust mass, TAC (Total Air Content), $\delta^{13}\text{C-CH}_4$. At the top the AICC2012 gas age (upper top axis) and the GICC05 ice age (lower top axis) of the respective depth are indicated. The mineral dust record is taken from Ruth et al. (2003), the Ca^{2+} record from Erhardt et al. (2022). The data overview for all further measured NGRIP bags can be found in Appendix A.

hat gelöscht: the

2.2 CH_4 , C_2H_6 , C_3H_8 and $\delta^{13}\text{C-CH}_4$ Analysis of Ice Core Samples

The short-chain alkanes and $\delta^{13}\text{C-CH}_4$ were measured at the University of Bern using the discrete wet extraction technique described in Schmitt et al. (2014). With this method, it is possible to measure mixing ratios of methane, ethane, and propane as well as the methane carbon isotopic signature and other trace gases on a single ice core sample of about 150 g.

hat gelöscht: as

hat gelöscht: in detail

Briefly, ice core samples are placed in a glass vessel locked by a stainless-steel flange which is attached to the vacuum line to evacuate laboratory air (see Fig. 3, step a). Before melting the ice sample, the leak tightness of the vacuum extraction line is tested with a so-called He blank. The ice sample is then melted under vacuum with the help of infrared radiation for ~35 min to release the enclosed air (step b). The released air is continuously removed from the sample

280 vessel by a pressure gradient towards an adsorbing AirTrap (activated carbon), collecting all
281 relevant air components at -180°C. After melting is completed, the temperature of the meltwater
282 is stabilized close to 0°C, but does not refreeze again. Afterwards, He is sparged with 4 mL/min
283 at standard temperature and pressure (equivalent to 100-400 mL at the varying low pressure in
284 the headspace) through the melt water for ~14 min through a capillary at the bottom of the
285 vessel to transfer any remnant gas species dissolved in the melt water onto the AirTrap (step c).
286 The sample vessel is then isolated by closing the inlet and outlet valves (step d). Consecutively,
287 the AirTrap is warmed up in two steps to first remove N₂ and O₂ and in a second step to release
288 the gases of interest which are then sent after a cryofocus step to the gas chromatograph (GC)
289 for separation and quantification using an isotope ratio mass spectrometer (Isoprime 100,
290 Elementar).

hat gelöscht:

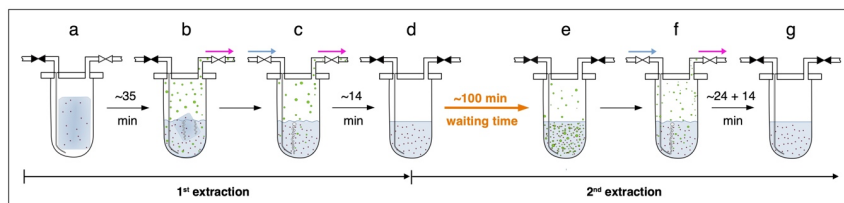
291
292 Precision of this method for CH₄ is about 8 ppb and 0.1 ‰ for δ¹³C-CH₄ based on the
293 reproducibility of the 1st extraction of ice core samples where isotopic data are expressed using
294 the δ notation on the international Vienna Pee Dee Belemnite (VPDB) scale. For C₂H₆, the
295 precision is 0.02 ppb or 1 ‰, for C₃H₈, 0.03 ppb or 5 ‰ (whatever is higher) based on the
296 reproducibility of standard air samples which are by definition not subject to excess production
297 (Schmitt et al., 2014). Blank levels for these species based on melted artificial (gas-free) ice
298 samples are 1-2 ppb for CH₄, 0.3 ppb for C₂H₆ and 0.2 ppb for C₃H₈ (Schmitt et al., 2014),
299 which are below the values measured on Antarctic ice, where excess production is minimal
300 compared to glacial Greenland samples (see Appendix B for details).

hat gelöscht: scaled

301
302 With their experimental investigations, Lee et al. (2020) were already able to demonstrate that
303 production/ release of CH_{4(x)s} is time-dependent. We therefore conclude that this process does
304 not have to be completed in the time available for the gas extraction described above. We
305 continued the analyses of excess alkane production with an additional extraction step (here
306 referred to as 2nd extraction, steps d-g in Fig. 3) following the normal ice extraction routine.
307 After all sample air is collected in the 1st extraction, the meltwater is left in the isolated sample
308 vessel (the vessel is closed and not connected to the carbon trap) and held at temperatures close
309 to 0°C for ~100 min (step d). After this “waiting time” of ~100 min, He is purged through the
310 meltwater for ~24 min to extract the gases that have been accumulated during this time interval
311 simulating the extraction time of the 1st extraction, followed by another ~14 min of He purging
312 to mimic the last step of the ice extraction when the sample had completely melted (step f). The
313 gases from this 2nd extraction are collected and measured following the same trapping and

hat gelöscht:

317 separation steps as in the 1st extraction. Note that the procedure of the 2nd extraction can be
 318 repeated any number of times (e.g. 3rd extraction).
 319
 320 The amount of gases that we obtain from the 1st extraction comprises the atmospheric amount,
 321 a possible contribution by in situ production, and a potential time-dependent production/release
 322 in the meltwater (*in extractu*). The 2nd extraction, however, targets only the *in extractu* fraction.
 323 The system blank for the 2nd extraction was estimated using the 2nd extraction of Antarctic ice
 324 (Talos Dome, EDC) and were 2 ppb, 0.3 ppb and 0.3 ppb for CH₄, C₂H₆ and C₃H₈, respectively,
 325 assuming an ice core sample air volume of 14 mL at standard temperature and pressure, which
 326 is the typical ice sample size of 150 g with a total air content of 0.09 mL/g. For CH₄ this is <
 327 1% of the amount of extracted species in the 1st extraction of glacial Greenland ice. Due to the
 328 small amount of CH₄ analyzed in this 2nd extraction (about a factor of 20 to 50 less than for an
 329 ice core sample) the precision for the $\delta^{13}\text{C}$ analysis is much lower than for the 1st (ice sample)
 330 extraction and we estimate the precision of $\delta^{13}\text{C}$ -CH₄ to 2 ‰ and for [CH₄] to be 2 ppb or 10
 331 ‰ (based on the reproducibility of 2nd extractions of Antarctic EDC samples). For C₂H₆ and
 332 C₃H₈, the precision is comparable to the 1st extraction. Note that throughout the manuscript we
 333 do not perform blank corrections (neither for the measured alkane concentrations nor for the
 334 isotopic values). The only exception is for the calculation of the temporal dynamics of excess
 335 ethane production (see Appendix C) as the blank contribution would otherwise bias the samples
 336 with low Ca²⁺ content.



339
 340 **Figure 3: Sequential steps (a-g) happening in the ice core sample vessel during the 1st and the 2nd extraction**
 341 **in the $\delta^{13}\text{C}$ -CH₄ extraction line.** Scheme illustrates the subsequent steps as described in detail in the text.
 342 Brownish spots indicate dust particles in the ice/ meltwater. Green circles indicate gas species (methane, ethane,
 343 and propane) in the meltwater or in the headspace of the vessel. Closed valves are indicated in black, open valves
 344 in white. Blue arrows indicate the He flow through the inlet capillary into the sample vessel, pink arrows indicate
 345 the flow direction from the sample vessel towards the AirTrap.

348 2.3 $\delta\text{D-CH}_4$ Analysis of Ice Core Samples

349 All $\delta\text{D-CH}_4$ data presented here were measured at the University of Bern using the discrete wet
350 extraction technique described in Bock et al. (2010a, 2014). This $\delta\text{D-CH}_4$ device allows to
351 measure the concentration of methane and its deuterium isotopic signature ($\delta\text{D-CH}_4$) on a single
352 ice core sample of about 300 g.

353
354 Briefly, ice core samples are melted after evacuation of the headspace using a warm water bath
355 at 40°C for 25–30 min to release the enclosed air into the sample vessel headspace. Once all the
356 ice is melted, the warm water bath is replaced by an ice-water bath to keep the meltwater
357 temperature and water vapor pressure low but without refreezing. In contrast to the $\delta^{13}\text{C-CH}_4$
358 method, the inlet and outlet valves are closed during the melting process. The released air leads
359 to an increased pressure in the sample vessel headspace enhancing the solubility of gases in
360 water. After the melting is complete, the inlet and outlet valves are opened and He is purged
361 for ~ 40 min with a flow of 360 mL/min to transfer the accumulated air in the headspace and
362 bubble He through the meltwater to strip dissolved gases. Just like for the $\delta^{13}\text{C-CH}_4$ method,
363 the air is collected on an activated carbon trap followed by further purification steps including
364 GC separation. Note that compared to the $\delta^{13}\text{C-CH}_4$ device, we performed only one extraction
365 with the $\delta\text{D-CH}_4$ device.

366
367 For both methods, we assume that the time for an *in extractu* production during the ice
368 extraction procedure starts with the first presence of meltwater until He purging is stopped.
369 Note that this time is considerably longer for the $\delta\text{D-CH}_4$ analysis (~ 60 min) compared to the
370 time of the 1st extraction in the $\delta^{13}\text{C-CH}_4$ analysis (~ 35 min).

371
372 Using this method we can measure $[\text{CH}_4]$ and $\delta\text{D-CH}_4$ with a precision of about 15 ppb and 3
373 ‰ (based on standard ice sample measurements), where isotopic data are expressed using the
374 δ notation on the international Standard Mean Ocean Water (SMOW) scale.

375 376 377 3. Characterization of excess alkanes in ice cores

378 3.1 Methane, ethane, propane concentrations

379
380 As described in detail in Sect. 2.2 a full ice sample measurement includes the regular ice sample
381 extraction (1st extraction) and, after the waiting time of ~ 100 min, a 2nd gas extraction in the
382 meltwater. Gas from the 1st extraction comprises atmospheric air, a possible contribution from

hat gelöscht: as

hat gelöscht: in detail

hat gelöscht: Note

hat gelöscht: ,

hat gelöscht: l

hat gelöscht: i

hat gelöscht: is comprised of

390 in situ production, a potential time-dependent contribution by an *in extractu* process, and any
391 contribution from the device itself (blank). For the gas species discussed here (methane, ethane,
392 propane), these individual fractions are very different in magnitude. For polar ice core samples,
393 the atmospheric air is the major fraction of methane even in dust-rich, glacial ice from
394 Greenland prone to CH_{4(xs)} production (see below). The opposite is expected for ethane and
395 propane, which are dominated by the *in extractu* component in dust-rich Greenland ice. To
396 establish a better knowledge of alkanes in Greenland ice, we evaluated the measured
397 concentrations of methane, ethane, and propane, their ratios to each other and the relation to the
398 content of mineral dust in the ice for both the 1st and the 2nd extraction.

399
400 Note that different units to indicate concentrations of the trace gases of interest are used
401 throughout this study. By using mixing ratios in units of [ppb], as typically used for atmospheric
402 concentrations, the concentration of trace gases is related to the amount of air extracted from,
403 the ice. Ice core samples with a low air content cause higher mixing ratio values for any
404 additional molecules produced in situ or *in extractu* compared to ice core samples with a high
405 air content and the interpretation might be biased. Alternatively, for any additional molecules
406 produced in situ or *in extractu*, [mol absolute per sample] denotes the absolute amount of trace
407 gases and is independent of the ice core air content. In the following, both units are used and
408 great care has to be taken to avoid misinterpretation of the results with respect to the different
409 units.

410
411 **3.1.1 Excess alkanes in the 1st extraction**

412
413 Figure 4 and 5 show results from the 1st extraction of our NGRIP and GRIP ice core samples.
414 For dust-rich samples, ethane ranges between 2 ppb and 12 ppb, and propane concentrations
415 between 1 ppb and 5 ppb. In contrast, low-dust samples from both GRIP and NGRIP have much
416 lower concentration (ca. 0.5 ppb for ethane, and 0.3 ppb for propane) consistent with estimates
417 of past atmospheric ethane and propane concentrations from the 15th to 19th century of the
418 common era being about 0.4 ppb in Greenland ice (Nicewonger et al., 2016) and lower for
419 propane (Helmig et al., 2013). Emissions of ethane and propane were likely reduced during the
420 glacial (Bock et al., 2017; Nicewonger et al., 2016; Dyonisius et al., 2020) thus, 0.5 ppb appears
421 to be an upper limit of past atmospheric concentrations of ethane and propane. This estimate of
422 past atmospheric ethane concentrations is an order of magnitude smaller than the values we
423 obtained from our dust-rich ice core samples from the 1st extraction, pointing to a strong

hat gelöscht: included in

425 additional source of these alkanes for dust-rich samples. Thus, the unusually high mixing ratios
426 indicate that ethane and propane in glacial ice extracted using our melt technique on discrete
427 samples do not represent atmospheric levels.

428

429 As illustrated in Fig. 4 (left panel), the ethane and propane concentrations are highly correlated,
430 pointing to a common production of excess ethane and excess propane. The weighted mean
431 ratio and its weighted standard deviation (both weighted according to the number of samples
432 measured per bag) is (2.25 ± 0.09) ppb ethane/ ppb propane. Note that all regression lines are
433 calculated by following the method of York (1968) and York et al. (2004). York's analytical
434 solution to the best-fit line accounting for normally distributed errors both in x and y is widely
435 used to determine an isotopic mixing line and has been proven as the least biased method (Wehr
436 and Saleska, 2017; Hoheisel et al., 2019). Throughout the manuscript we use the 1 sigma (1σ)
437 standard deviation to express uncertainties. In Fig. 4, where the individual bags studied are
438 color-coded, we can clearly see that the ratio is essentially the same between the individual bags
439 and that the correlation is also very high within each bag (although we have to consider for the
440 significance of this correlation that the number of samples per bag is very low). This indicates
441 that for NGRIP ice ethane and propane are found in a fixed ratio. Accordingly, excess ethane
442 and propane production can be well represented by the weighted mean ratio and ethane and
443 propane are produced in a ratio of approximately 2:1. Very similar results were also observed
444 in NGRIP samples measured in 2011 and in GRIP samples revealing an ethane to propane ratio
445 of 2.14 ± 0.03 ($r^2 = 0.99$) and 2.00 ± 0.13 ($r^2 = 0.99$), respectively (see Fig. 4, left panel).

hat gelöscht: s

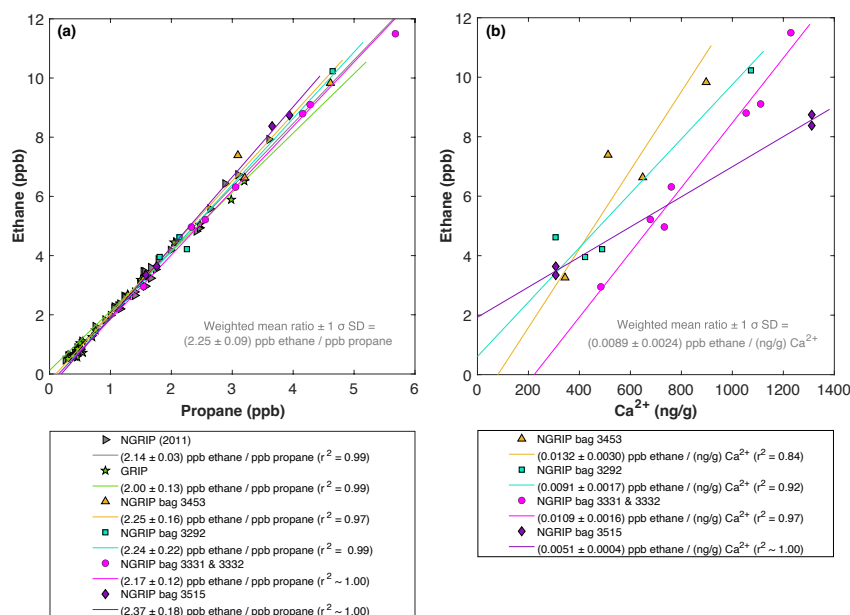


Figure 4: NGRIP and GRIP results of ethane and propane from the 1st extraction. (a) Concentrations of ethane and propane and their ratios to each other for NGRIP and GRIP samples measured in the 1st extraction of the $\delta^{13}\text{C}$ -CH₄ device. Colors and symbols indicate the different NGRIP bags or cores used. (b) Bag-specific production ratios of ethane in relation to the Ca^{2+} concentration for NGRIP samples. Note that for bag 3515 there is a data gap in the Ca^{2+} record and an anomaly of the Ca^{2+} to dust mass ratio for the replicate sample at 1932.7 m. Thus, the Ca^{2+} concentration for these two data points is likely overestimated (see Fig. A3).

hat gelöscht:

Methane concentrations range from 407 ppb to 476 ppb and are predominantly of atmospheric origin (see Fig. 5). The amount of $\text{CH}_{4(\text{xs})}$ is the difference between the measured methane concentration and the atmospheric background concentration. To quantify $\text{CH}_{4(\text{xs})}$ we use the fact that due to the low-pass filtering of the bubble enclosure process all samples within one bag should have the same atmospheric CH_4 concentration. This also ensures that any physical processes that potentially influence the atmospheric alkanes in our samples (gravitational enrichment, thermodiffusion, disequilibrium effects on CH_4 isotopes) are the same for all samples within one bag. The only difference between these samples is, thus, the degree of $\text{CH}_{4(\text{xs})}$ production which can be estimated from the linear fit between the measured CH_4 concentration and the concentration of another species (e.g. ethane, propane, mineral dust, or Ca^{2+}), which serves as a proxy for $\text{CH}_{4(\text{xs})}$ production. The closest relationship was found for $[\text{C}_2\text{H}_6]$ and quantifying $\text{CH}_{4(\text{xs})}$ was done by extrapolating the linear regression between ethane

469 and methane to an ethane concentration of 0.39 ppb, the assumed atmospheric [C₂H₆]. This
470 leads to an estimate of the true atmospheric [CH₄] value within the respective bag, a value that
471 can then be subtracted from the measured CH₄ concentration to obtain the CH_{4(x)s} in each
472 sample. The uncertainty of the calculated CH_{4(x)s} is typically 8 ppb.

473

474 Using the relation of ethane to methane this approach translates into CH_{4(x)s} in the range of 14
475 ppb to 91 ppb for these five NGRIP bags with a mean excess of 39 ppb. Equivalent calculations
476 can be made using propane, dust, or Ca²⁺ as proxy for CH_{4(x)s} production, however, the
477 relationship between dust parameters and CH_{4(x)s} is more variable and does not lead to equally
478 precise values for CH_{4(x)s}. Nevertheless, the obtained mean CH_{4(x)s} using the relation of mineral
479 dust or Ca²⁺ to methane is similar in size to the one obtained by ethane.

480

481 We find a constant production ratio between all three excess alkanes for all bags investigated.
482 The weighted mean production ratio and its weighted standard deviation was calculated to be
483 (6.42 ± 1.57) ppb methane / ppb ethane and (14.3 ± 3.7) ppb methane/ ppb propane for the
484 samples of the five main NGRIP bags, and (2.25 ± 0.09) ppb ethane/ ppb propane (also
485 including NGRIP2011 and GRIP here). Note that there is a flagged sample for CH₄ in bag 3453
486 (yellow asterisk in Fig. 5), where one vent (V6) was unintentionally open during the
487 measurement, which may have compromised the result. We, therefore, excluded the production
488 ratio determined from bag 3453.

489

490 In summary, we can characterize the excess alkane production in our measured NGRIP samples
491 by an overall methane/ethane/propane ratio of approximately 14:2:1. This constant relationship
492 between different alkanes suggests that excess alkanes are produced in a fixed ratio by a
493 common production process.

494

495 Another important observation is the close relation between excess alkanes and the content of
496 mineral dust within the ice core samples. Using measurements on GISP2 and NEEM ice core
497 samples, Lee et al. (2020) reported for the first time the close relation of CH_{4(x)s} to chemical
498 impurities with the highest correlation with Ca²⁺. This is supported by our measurements on
499 NGRIP and GRIP samples revealing an overall increase of CH_{4(x)s}, ethane, and propane with
500 increasing Ca²⁺ (see for example the ethane/Ca²⁺ relationship in Fig. 4, right panel). Although
501 the connection between ethane and Ca²⁺ is more variable than for ethane and propane between
502 the different bags, the slopes of the linear regressions in Fig. 4 (right panel) are still the same

hat gelöscht: that there exists

hat gelöscht: therefore

hat gelöscht: ,

hat gelöscht: ,

507 within the 2σ uncertainty and the weighted mean ratio of all NGRIP samples amounts to
508 (0.0089 ± 0.0024) ppb ethane/ (ng/g) Ca^{2+} . However, this weighted mean value is likely biased
509 low due to the relatively low ethane/ Ca^{2+} slope of bag 3515. Due to a data gap at 1932.7 m in
510 the Ca^{2+} record, the corresponding Ca^{2+} concentration for two of the samples of this bag is
511 subject to a large interpolation error and overestimated Ca^{2+} (see Fig. A3).

512

513 The results agree with results from GRIP and [earlier](#) NGRIP (2011) [measurements](#), revealing
514 an ethane/ Ca^{2+} ratio of 0.0105 ± 0.0029 ($r^2 = 0.76$) and 0.0090 ± 0.0006 ($r^2 = 0.91$),
515 respectively.

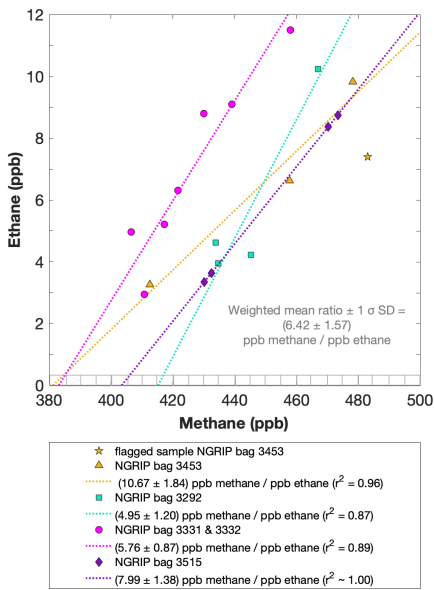
516 Based on the fixed ratio of $\text{CH}_4(\text{xs})$ and ethane described above this translates into a weighted
517 mean excess $\text{CH}_4/\text{Ca}^{2+}$ ratio of (0.0529 ± 0.0111) ppb methane per (ng/g) Ca^{2+} .

518

hat gelöscht: older

hat gelöscht: samples

hat gelöscht: excess CH_4



519

520 **Figure 5: NGRIP results of methane and ethane from the 1st extraction.** Concentrations of methane (ppb) and
521 ethane (ppb) and their ratios to each other for NGRIP samples measured in the 1st extraction of the $\delta^{13}\text{C}-\text{CH}_4$
522 device. Different colors and symbols indicate the different NGRIP bags used for our analysis. Note that there is a
523 flagged sample for CH_4 in bag 3453 as indicated with a yellow asterisk, which is not included in the ratio of bag
524 3453. The grey hatched area indicates past atmospheric ethane concentrations of maximum 0.39 ppb as estimated
525 by Nicewonger et al. (2016).

526

527

528

532 3.1.2 Excess alkanes in the 2nd extraction

533

534 With the 2nd extraction of the $\delta^{13}\text{C}$ -CH₄ analyses we can evaluate the temporal dynamics of
535 excess alkane production, assuming that all alkanes extracted in the 2nd extraction were
536 produced after the 1st extraction was completed.

hat gelöscht: in the

hat gelöscht: time

537 For our Greenland samples we measured a range of about 0.2 to 2.4 pmol for ethane and a range
538 of 0.1 to 1.2 pmol for propane in the 2nd extraction (Fig. 6, right panel). These values in pmol
539 are equivalent to 0.2 to 4.8 ppb of ethane and 0.2 to 2 ppb of propane assuming that the amount
540 of excess alkanes was added to 14 mL of ice core air (which is the typical ice sample size of
541 150 g with a total air content of 0.09 mL/g). The measured amount of methane ranges between
542 3 pmol and 20 pmol (Fig. 6, left panel).

543

544 The ratio of the measured amount for the individual species between the 1st and the 2nd
545 extraction amounts to 3.6 ± 0.85 ($r^2 = 0.78$) for ethane (Fig. 7, right panel), 3.3 ± 0.33 ($r^2 =$
546 0.78) for propane (combined data of NGRIP and GRIP) and 3.8 ± 1.62 ($r^2 = 0.33$) for methane
547 (only NGRIP data), where the uncertainty for CH₄ is again much larger. Thus, we can conclude
548 that the amount of alkanes produced during the waiting time after the 1st extraction until the 2nd
549 extraction was finished, was approximately 30% of the amount produced during the 1st
550 extraction. Results from the 2nd extraction also demonstrate that this process is slow and not
551 completed during the 1st extraction. We can thereby confirm the results of Lee et al. (2020) but
552 we are able to show for the first time that this process leads also to production of excess ethane
553 and propane.

hat gelöscht: time of the

554

555 For a better estimate of the temporal reaction kinetics of the underlying process, we can relate
556 the measured amount of the individual species to the time available for a potential reaction in
557 the meltwater during each extraction. For the five GRIP samples that were measured with a 2nd
558 and 3rd extraction (see Sec. 2.2 for details) we take the cumulative production amount (where
559 the first data point is the produced amount in the 1st extraction, the second data point is the sum
560 of the 1st and 2nd extraction, and the third data point is the sum of the 1st, 2nd, and 3rd extraction).

561 In the example shown for ethane (Fig. C1, Appendix C), we can see the assumed first-order
562 reaction kinetics with a decreasing ethane accumulation over time providing a good model for
563 our measurements (details on the calculation can be found in Appendix C). With that, we can
564 estimate the half-life time (τ) of the production to be approximately 30 min. Note that this long
565 half life has also an implication for a potential excess production of CH₄ in continuous flow

hat gelöscht: saturation of

hat gelöscht: the

571 techniques, where the time before the air is separated from the liquid water stream is only 1-2
572 min. Thus, only 5-10 % of the *in extractu* production found in our 1st extraction can be expected
573 in such continuous flow techniques, which are difficult to detect.

hat gelöscht: reaction

hat gelöscht: measurements

574
575 The goodness of fit of the ratios of the measured concentrations between the 1st and the 2nd
576 extraction is $r^2 = 0.78$ for both ethane and propane, indicating that the production/release in the
577 1st extraction in relation to the 2nd extraction is well correlated for both species (see Fig. 7b for
578 ethane). Thus, samples that produced higher excess alkanes during the 1st extraction also
579 produced more excess alkanes in the 2nd extraction, suggesting that the production is dependent
580 on the amount of some reactant present in the samples from which excess alkanes are produced.
581 Again, for CH₄ this relationship is more variable which is likely related to the higher uncertainty
582 in measuring CH₄ for the 2nd extraction.

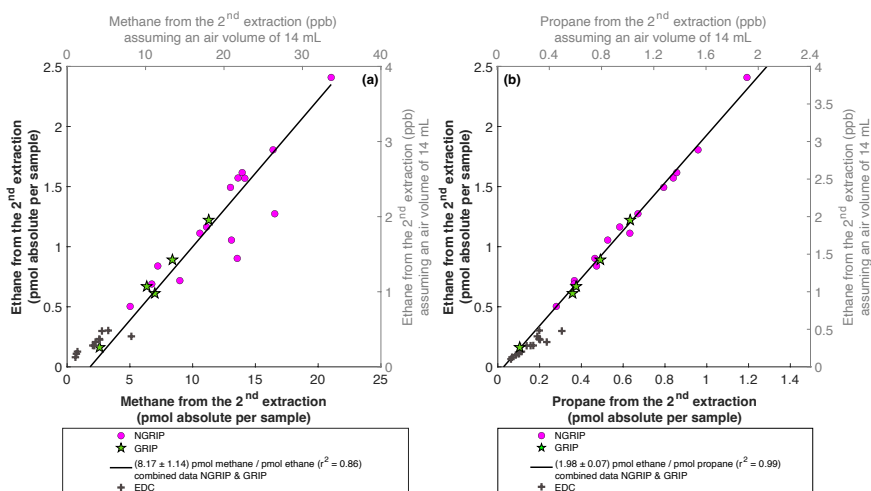
583
584 The ratio of ethane to propane of all measured Greenland samples in the 2nd extraction is 1.98
585 ± 0.07 ($r^2 = 0.99$). The ratio of methane to ethane is 8.17 ± 1.14 ($r^2 = 0.86$). Accordingly, the
586 overall relationship between methane, ethane, and propane in the 2nd extraction can be
587 characterized by a ratio of approximately 16:2:1. However, comparing the ratios of
588 ethane/propane and methane/ethane between the 1st and the 2nd extraction, there is no significant
589 difference within the 2σ uncertainties from 2.25 ± 0.09 to 1.98 ± 0.07 , and from 6.42 ± 1.57 to
590 8.17 ± 1.14 . We can conclude that within the error limits, the production ratios stayed the same,
591 suggesting that the same *in extractu* process is at play during both extractions.

592
593 In the 2nd extraction, we can again observe the relation between excess alkanes and the amount
594 of mineral dust. Figure 7a shows the correlation of ethane (fmol/g meltwater) to Ca²⁺ (ng/g) in
595 all measured NGRIP and GRIP samples in the 2nd extraction revealing a production of $(0.0085$
596 $\pm 0.0011)$ fmol/(g meltwater) ethane per (ng/g) Ca²⁺ with $r^2 = 0.70$. For methane, we observe a
597 production ratio of (0.0556 ± 0.01513) fmol/(g meltwater) methane per (ng/g) Ca²⁺ with a
598 correlation of $r^2 = 0.47$ (data not shown).

599
600 Overall, excess alkane concentrations increase with increasing Ca²⁺ concentrations, in both the
601 1st and the 2nd extraction. The total alkane production/release, however, decreased in the 2nd
602 extraction, suggesting the progressive exhaustion over time of some reactant necessary for the
603 *in extractu* process. We propose that this reactant co-varies with Ca²⁺ and particulate dust,

hat gelöscht: are increasing

607 where Ca^{2+} is of course not a reactant itself and represents only a proxy for higher *in extractu*
 608 production.
 609



610
 611 **Figure 6: NGRIP and GRIP results of excess methane, ethane, and propane from the 2nd extraction. (a)**
 612 **Concentrations of methane and ethane and their ratios to each other. (b) Concentrations of propane and ethane and**
 613 **their ratios to each other. Units are given as pmol absolute per sample on the primary axis in black and in ppb**
 614 **assuming an air volume of 14 mL of the ice core sample on the secondary axis in grey. Crosses indicate the blank**
 615 **level of the system estimated from 2nd extractions of EDC ice core samples.**

hat gelöscht: Grey

hat gelöscht: c

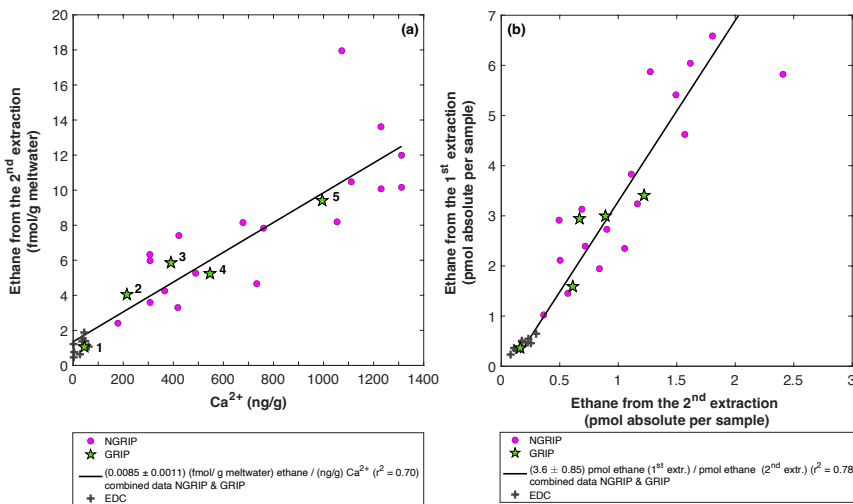


Figure 7: **GRIP and GRIP results of ethane from the 2nd extraction in relation to the Ca²⁺ concentration and to the 1st extraction.** (a) Produced amount of ethane in the meltwater (fmol/g meltwater) in relation to the Ca²⁺ concentration in the ice core samples. The numbered GRIP samples are used in Figure C1 to evaluate the temporal dynamics. Crosses indicate the blank level of the system estimated from 2nd extractions of EDC ice core samples. (b) Relation of the amount of ethane (pmol) measured in the 1st and 2nd extraction.

3.2 Isotopic composition of excess methane

In this section we characterize the isotopic signature of excess methane and explore how we can use this parameter to better identify its source or production pathway. The evaluation of the carbon and deuterium isotopic signature of excess methane ($\delta^{13}\text{C-CH}_4(\text{xs})$ and $\delta\text{D-CH}_4(\text{xs})$) is based on the Keeling-plot approach (Keeling, 1958, 1961; Köhler et al., 2006).

3.2.1 $\delta^{13}\text{C-CH}_4$ isotopic signature of excess methane

Figure 8 (left panel) shows the $\delta^{13}\text{C-CH}_4$ results of the 1st extraction. The carbon isotopic signature of excess CH₄ from the 1st extraction of the ice core sample measurements within one NGRIP bag are obtained from the y-intercept of the Keeling-plot, representing the excess $\delta^{13}\text{C-CH}_4$ value for this bag. Note that the two NGRIP bags 3331 and 3332 are neighbouring bags and were therefore combined into one Keeling y-intercept. As the individual samples in these two bags span less than 10 years between each other, they are the same within the age distribution, and the assumptions for the Keeling-plot approach (see Sec. 2.1) are met. All bags show agreement in $\delta^{13}\text{C-CH}_4$ signature (y-intercepts) within 2 σ uncertainties. The weighted

hat gelöscht: 7

hat gelöscht: Grey

hat gelöscht:

hat gelöscht: c

650 mean isotopic signature is $(-47.0 \pm 2.9) \text{ ‰}$, with weights assigned by the number of samples
651 that constrained each individual Keeling plot regression line.

652 With the small number of samples that go into the determination of the y-intercept and its error
653 in the Keeling plot for each individual bag, the estimates of the y-intercepts and their error have
654 to be regarded statistically uncertain. However, comparing the results for the individual bags,
655 they all agree within each within the estimated errors. In order to get a more representative
656 value for the isotopic signature of excess CH_4 and its error, we calculate a weighted average
657 for all bags for the y-intercept and its error. Nevertheless, this weighted error may still not be
658 entirely representative because of the small sample number and the true error may likely be
659 somewhat higher.

660
661 Figure 8 (right panel) shows the isotopic results in relation to the amount of CH_4 produced
662 during the 2nd extraction. No atmospheric CH_4 is present during the 2nd extraction and the
663 individual isotopic values in Fig. 8 (right panel) are the directly measured values of excess CH_4
664 without applying the Keeling-plot approach. For a better comparison, the produced CH_4 is
665 shown both in pmol (lower axis in Fig. 8, right panel) and in a mixing ratio CH_4 scale (ppb).
666 The Keeling y-intercept values of the 1st extraction are added in the right panel of Fig. 8.

667
668 The $\delta^{13}\text{C}$ - CH_4 values of the 2nd extraction range between -34 ‰ and -48 ‰ with the mean being
669 $(-41.2 \pm 2.2) \text{ ‰}$. This value appears isotopically somewhat heavier compared to the weighted
670 mean of $(-47.0 \pm 2.9) \text{ ‰}$ inferred from the Keeling analysis, however, is still the same within
671 the 2σ error limits. We note that the measured peak areas for the 2nd extractions are very small
672 and lie outside of the typical range of our gas chromatography mass spectrometry analysis for
673 $\delta^{13}\text{C}$ - CH_4 and we cannot exclude some bias in these results. However, we mimicked these small
674 peak areas with injections of small amounts of standard air and observed no significant bias in
675 the measured $\delta^{13}\text{C}$ - CH_4 values given that the precision of such small peaks is around 2 ‰ .

676
677 Another caveat is the considerable blank contribution for CH_4 that we observe for the 2nd
678 extraction. Since Antarctic ice cores do not show a sizable *in extractu* production (Fig. 7,
679 crosses for EDC) we measured EDC samples with the same protocol of a 2nd extraction as for
680 our Greenland samples to provide an upper boundary of this blank. Hence the 2nd extraction of
681 the EDC samples are a conservative blank estimate while the true system blank is lower. As
682 can be seen in Fig. 8 (right panel) the amount of CH_4 measured for these EDC samples (crosses)
683 is on average about 2 pmol (equivalent to about 3 ppb). For comparison, our ice samples from

hat gelöscht: "

hat formatiert: Schriftart: (Standard) Times New Roman

hat gelöscht: t

hat gelöscht: "

hat gelöscht: ¶

hat gelöscht: grey

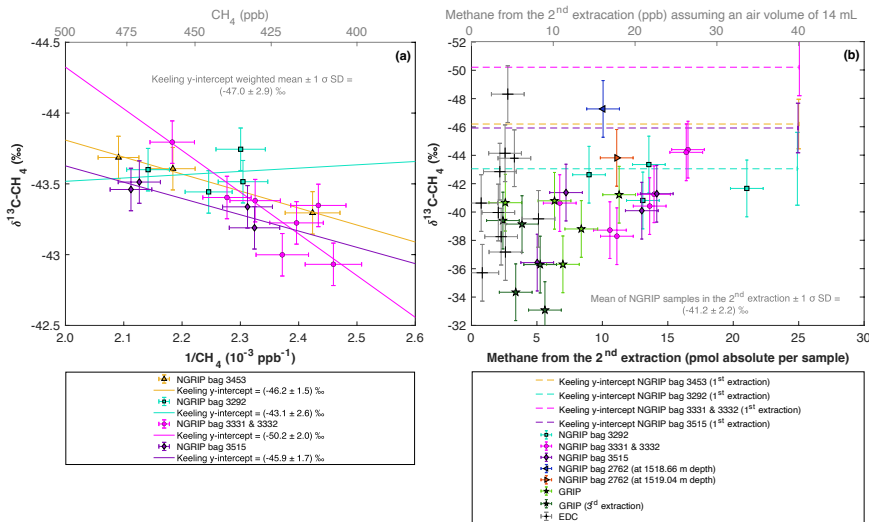
hat gelöscht: grey

Greenland show a range of about 5 to 20 pmol, indicating a considerable blank contribution in the 2nd extraction.

692

To estimate the influence of the blank on the isotopic signature that occurs during the 2nd extraction we used the values from our EDC measurements and applied an isotope mass balance approach. The $\delta^{13}\text{C}-\text{CH}_4$ blank signature obtained from these EDC samples is -39.0 ‰, hence a few ‰ heavier than the mean $\delta^{13}\text{C}-\text{CH}_4$ signature of the excess CH_4 from this 2nd extraction for the Greenland samples. On average, the correction would shift our NGRIP values towards lighter (more negative) values by 0.31 ‰. This systematic correction is thus small compared to the typical measurement precision obtained both from the Keeling-plot approach and the direct measurement of the $\text{CH}_{4(\text{xs})}$ with the 2nd extraction. As the $\delta^{13}\text{C}-\text{CH}_4$ signature of the blank is close to the NGRIP values, performing a blank correction has only little leverage. Considering these analytical limitations of our 2nd extraction for $\delta^{13}\text{C}-\text{CH}_4$, these findings suggest that $\text{CH}_{4(\text{xs})}$ produced during the 1st and 2nd extraction has the same $\delta^{13}\text{C}-\text{CH}_4$ isotopic signature within the 2 σ error limits and is likely produced/released by the same process in both extractions.

706



707

708 **Figure 8: NGRIP (and GRIP) $\delta^{13}\text{C}-\text{CH}_4$ results of the 1st and 2nd extraction measured with the $\delta^{13}\text{C}-\text{CH}_4$**
 709 **device. (a) Keeling-plot of $\delta^{13}\text{C}-\text{CH}_4$ for NGRIP samples from the five main bags (3292, 3331 & 3332, 3453,**
 710 **3515) measured in the 1st extraction. Colors and symbols indicate individual measurements of the respective bags.**
 711 **Colored lines indicate the corresponding Keeling regression line of each individual bag. (b) $\delta^{13}\text{C}-\text{CH}_4$ (‰) values**
 712 **in relation to the amount of methane measured for the 2nd extraction. Units for CH_4 are given as pmol absolute per**
 713 **sample on the primary axis in black, and in ppb assuming an air volume of 14mL of an ice core sample on the**
 714 **secondary axis in grey. Colors and symbols indicate individual measurements of the respective bags. Color-coded**

715 lines indicate the corresponding Keeling y-intercept of each individual bag as measured in the 1st extraction. Grey
716 crosses indicate the blank level of the system estimated from 2nd extractions of EDC ice core samples.

717

718 3.2.2 $\delta\text{D-CH}_4$ isotopic signature of excess methane

719

720 Figure 9 shows the results of the $\delta\text{D-CH}_4$ analyses. Due to the larger sample size required for
721 the $\delta\text{D-CH}_4$ analyses and the sample availability restrictions, only two bags could be measured
722 for $\delta\text{D-CH}_4$. The individual $\delta\text{D-CH}_4$ results obtained from the ice core sample measurements
723 within one NGRIP bag are again combined into one Keeling y-intercept, representing the $\delta\text{D-CH}_4$
724 value for this bag. NGRIP bag 3460 (orange) reveals a Keeling y-intercept $\delta\text{D-CH}_4$ value
725 of $(-308 \pm 51) \text{‰}$. The two NGRIP bags 3266 and 3267 (purple) are neighbouring bags and
726 were combined into one Keeling y-intercept revealing a $\delta\text{D-CH}_4$ value of $(-341 \pm 62) \text{‰}$. The
727 difference between the two Keeling y-intercepts is within the error limits. Accordingly, we
728 combine the two values to a weighted mean and weighted uncertainty of $(-326 \pm 57) \text{‰}$. As
729 stated above, with the small number of samples that go into the determination of the y-intercept
730 and its error in the Keeling plot for each bag, the estimates of the y-intercepts and their error
731 have to be regarded statistically uncertain.

732 Our results are consistent with the findings of Lee et al. (2020), who used the NGRIP $\delta\text{D-CH}_4$
733 record of Bock et al. (2010b) and the NGRIP $[\text{CH}_4]$ record of Baumgartner et al. (2014) to
734 estimate the $\delta\text{D-CH}_{4(\text{xs})}$ signature in these samples. Assuming a two-component mixture of
735 atmospheric methane and excess methane in their model led to a best estimate of (-293 ± 31)
736 ‰ for $\delta\text{D-CH}_{4(\text{xs})}$ which is within the error limits of our Keeling-plot results.

737

hat gelöscht: isotopic

hat gelöscht: studied

hat gelöscht: isotopic

hat gelöscht: therefore

hat gelöscht: of the individual bags

hat formatiert: Schriftart: (Standard) Times New Roman,
Schriftfarbe: Text 1

hat formatiert: Schriftart: (Standard) Times New Roman,
Schriftfarbe: Text 1, Englisch (USA)

hat gelöscht: individual

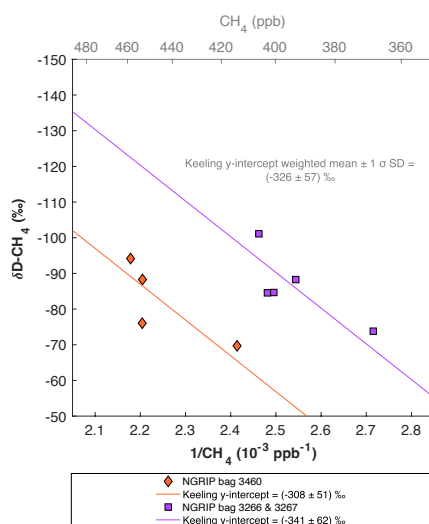


Figure 9: NGRIP $\delta\text{D-CH}_4$ results. Keeling-plot of $\delta\text{D-CH}_4$ of NGRIP samples measured with the $\delta\text{D-CH}_4$ device. Colors and symbols indicate individual measurements of the respective bags and lines indicate the corresponding regression of each bag.

hat gelöscht: colored

hat gelöscht: individual

4. Testing the hypotheses explaining excess alkanes

In Sect. 3 several pieces of evidence for the production/release of excess alkanes in Greenland ice core samples were collected:

- We can confirm the observations of Lee et al. (2020) on excess methane in different Greenland ice cores and its covariance with the amount of mineral dust in the ice. Despite the different extraction techniques applied (multiple melt-refreeze method in Lee et al. (2020) versus two subsequent wet extractions in our study), we can further corroborate that the temporal dynamics of the production/release is on the order of hours and production/ release occurs when liquid water is present during extraction.
- We document for the first time a co-production/release of excess methane, ethane, and propane, with the observed values for ethane and propane exceeding by far their estimated past atmospheric background concentrations.
- Excess alkanes (methane, ethane, propane) are produced/ released in a fixed molar ratio of approximately 14:2:1, indicating a common origin.

- We further characterize the isotopic composition of excess CH₄ of $\delta^{13}\text{C}-\text{CH}_{4(\text{xs})}$ and $\delta\text{D}-\text{CH}_{4(\text{xs})}$ to be $(-47.0 \pm 2.9) \text{ ‰}$ and $(-326 \pm 57) \text{ ‰}$ in NGRIP ice core samples, respectively. Within the error limits, our $\delta\text{D}-\text{CH}_{4(\text{xs})}$ results are consistent with the calculated best estimate of $(-293 \pm 31) \text{ ‰}$ by Lee et al. (2020).

In the introduction we presented the hypotheses proposed by Lee et al. (2020) explaining their observations on CH_{4(xs)}. Here we resume the discussion of the original hypotheses and refine them in light of our new data from NGRIP and GRIP measurements. An overview of the possible sources explaining excess alkanes is illustrated in Fig. 10 and Table 1. We discuss in the following three options for the origin of the observed excess alkanes:

1.) Excess alkanes could be adsorbed on mineral dust particles prior to their deposition on the Greenland ice sheet and released in the laboratory during the prolonged melting process. The adsorption step could happen in the mineral dust source region (East Asian deserts) thereby adsorbing the alkanes from natural gas seeps within the sediment (process marked as A1, see Fig. 10). Alternatively, adsorption of atmospheric alkanes on dust particles can happen anytime starting from the soil surface in the dust source region, during atmospheric transport to the Greenland ice sheet, or within the firm layer before pores are closed-off (A2). The desorption of the adsorbed alkanes happens during the melting process for both cases.

2.) Excess alkanes could be produced microbially. The production happens either in the ice (in situ), the alkanes are adsorbed on dust particles in the ice and then slowly released during the melting phase in the laboratory (M1). Alternatively, the microbial production happens in the meltwater during the melting process (*in extractu*) (M2). A microbial in situ production in the ice without an adsorption-desorption process was already deemed unlikely by Lee et al. (2020) since it is not compatible with the lack of CH_{4(xs)} in the CFA CH₄ concentration records.

3.) Excess alkanes are produced abiotically, e.g. by the decomposition of labile organic compounds. This chemical reaction can happen either in the ice (in situ), where excess alkanes are then adsorbed on dust particles and subsequently released during the melting process (C1), or in the meltwater during extraction (*in extractu*) (C2). An abiotic in situ production in the ice without an adsorption-desorption process can also be ruled out with the CFA evidence.

We now discuss these mechanisms in detail and evaluate the viability of the different hypotheses in light of our new experimental observations.

hat gelöscht: ice sample

hat gelöscht: different

hat gelöscht: after deflation

hat gelöscht: itself

hat gelöscht: ,

hat gelöscht: excess CH₄

hat gelöscht: i

hat gelöscht: itself

hat gelöscht: the

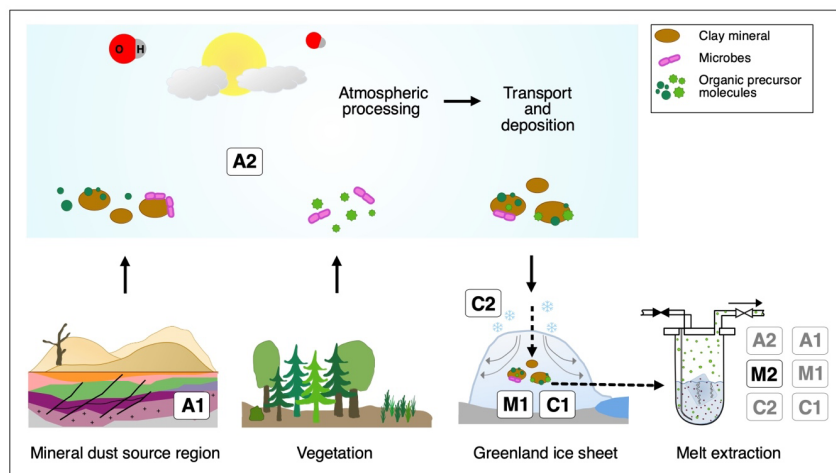


Figure 10: Overview of the different possibilities explaining excess alkanes in dust-rich Greenland ice. A depicts an adsorption process of alkanes on mineral particles, either from natural gas seeps within the sediment (A1) or from the atmosphere (A2) prior to their deposition on the Greenland ice sheet. This gas is then desorbed during melting in the laboratory. M depicts a microbial production of excess alkanes, either in the ice (*in situ*), followed by adsorption on dust particles in the ice and a subsequent slow desorption process during melting (M1), or a microbial production in the meltwater (*in extractu*) (M2). C depicts the abiotic/chemical production of excess alkanes, either in the ice (*in situ*) followed by adsorption on dust particles after production in the ice and a subsequent slow desorption during the melting process (C1), or an abiotic production in the meltwater (*in extractu*) (C2).

(1) Adsorption/desorption of alkanes on mineral dust particles

Depending on where the adsorption occurs, the mineral particles might adsorb alkanes of different origin and composition. One possibility is that the adsorption already takes place within the sediment or soil of the dust source region, thus before mineral dust deflation (erosion of loose material by winds from flat and dry areas; A1). As proposed by Lee et al. (2020), the major source region of mineral dust arriving in Greenland during the glacial (Taklamakan, Tarim Basin) are also regions where natural gas seeps reach the surface (Etiopie and Klusman, 2002; Etiopie et al., 2008). In this case, the measured excess alkanes should reflect the seep's isotopic and alkane composition. Alternatively, adsorption of atmospheric alkanes on the particles can happen anytime starting from the soil surface, during transport en route to the Greenland ice sheet after deflation, and within the firn layer before pores are closed-off (A2). For the scenario A2 the fingerprint (isotopic composition and ratio of alkanes) of the adsorbed alkanes depends on the past atmospheric composition but could be modulated by selective fractionation processes during adsorption and desorption.

hat gelöscht: the

hat gelöscht: process

hat gelöscht: itself

hat gelöscht: the

hat gelöscht: process

hat formatiert: Schriftart: Kursiv

hat gelöscht: itself

hat formatiert: Schriftart: Kursiv

hat gelöscht: takes place

hat gelöscht: the methane should reflect the isotopic composition and alkane composition of the seep

846

847 To be a viable mechanism for our problem, it requires that the adsorbed alkanes stay strongly
848 bound at the dust particles while desorption is minor both during the atmospheric transport and
849 during the several hundred years the dust particles spend in the porous firn (age of the firn at
850 bubble close-off). During the melting procedure the adsorbed alkanes would then be released
851 from their mineral dust carrier, which in case of Greenland ice from glacial times is
852 predominately consisting of clay minerals from the Taklamakan (and partly also Gobi) desert
853 (Biscaye et al., 1997; Svensson et al., 2000; Ruth et al., 2003). However, additional dust sources
854 exist, with their relative contribution varying with climate conditions (Han et al., 2018; Lupker
855 et al., 2010).

856

857 Several experimental studies showed that clay minerals have a high adsorption capacity and
858 retention potential for alkanes (Sugimoto et al., 2003; Cheng and Huang, 2004; Dan et al., 2004;
859 Pires et al., 2008; Ross and Bustin, 2009; Ji et al., 2012; Liu et al., 2013; Tian et al., 2017).
860 Influencing parameters for an adsorption-desorption process are mainly pressure, temperature,
861 clay mineral type, micropore size, surface area, organic carbon content, and water/ moisture
862 content (Sugimoto et al., 2003; Cheng and Huang, 2004; Dan et al., 2004; Pires et al., 2008;
863 Ross and Bustin, 2009; Ji et al., 2012; Liu et al., 2013; Tian et al., 2017). Most interestingly for
864 us, studies by Sugimoto et al. (2003) and Dan et al. (2004) on the adsorption of CH₄ in
865 micropores on the surface of clay minerals in dried and fresh lake sediment showed that dried
866 sediment still retains CH₄ and that dried and degassed sediment re-adsorbs ambient CH₄ at
867 standard pressure and room temperature. The amount of CH₄ adsorbed in their samples strongly
868 depends on pressure and temperature while increasing temperatures and decreasing pressure
869 lead to stronger desorption. The addition of water/ moisture leads to a rapid desorption of
870 already adsorbed gases (Sugimoto et al., 2003; Dan et al., 2004; Pires et al., 2008; Ji et al.,
871 2012; Liu et al., 2013).

872

873 These observations support the possibility of an adsorption-desorption process for our glacial
874 NGRIP and GRIP ice core samples, where alkanes (from fossil seeps or atmosphere) would be
875 adsorbed on dust particles and desorbed during the extraction when liquid water is present.
876 Independent of the origin of the alkanes (A1 or A2), the amount of alkanes adsorbed on dust
877 deposited onto the Greenland ice sheet by this process would be diminished if the dust particles
878 were already in contact with liquid water during the long-range transport which may lead to a
879 loss of previously adsorbed alkanes. This water contact could occur, for example, already at the

hat gelöscht: mineral

hat gelöscht: s

hat gelöscht: other

hat gelöscht: is strongly dependent

hat gelöscht: a

hat gelöscht: results

hat gelöscht: in principle

hat gelöscht: measurement procedure

hat gelöscht: mineral

hat gelöscht: already in the atmosphere

890 dust source, as it is known that the deserts in the Tarim basin receive regular input from water
891 from the surrounding mountain regions [that](#) also provide the minerals to the basin that are blown
892 out of the desert afterwards (Ruth et al., 2007).

hat gelöscht: ing

894 To explain the constant ratio of methane, ethane, and propane of 14:2:1 in our samples with an
895 adsorption mechanism, we need to discuss the potential origins of the adsorbed alkanes. First,
896 we find very high relative excess contributions of ethane and propane in our samples, while we
897 see a small excess contribution for methane compared to the atmospheric background. This is
898 not in line with the past atmospheric $\text{CH}_4/(\text{C}_2\text{H}_6+\text{C}_3\text{H}_8)$ ratio where past atmospheric ethane
899 concentrations by Nicewonger et al. (2016) are an order of magnitude smaller (and propane
900 concentrations even less) than the measured concentrations in [dust-rich Greenland ice core](#)
901 samples.

hat gelöscht: . If we assume a comparable adsorption for all three alkanes, this would

hat gelöscht: imply a strong relative enrichment of ethane and propane over methane in the concentration of these gases during adsorption.

hat gelöscht: our NGRIP and GRIP

902 In contrast, the ratio of methane, ethane, and propane for our samples of approximately 14:2:1,
903 translates into a $\text{CH}_4/(\text{C}_2\text{H}_6+\text{C}_3\text{H}_8)$ ratio of ~ 5 , which is most consistent with a thermogenic
904 origin (see Fig. 11, left panel). However, due to the different adsorption capacity of mineral
905 dust particles, also a fractionation of the three alkanes is to be expected during the adsorption
906 process, which could alter the thermogenic signature.

908 To further evaluate the adsorption theory in light of our experimental [results](#), we now include
909 the carbon and deuterium isotopic signature of $\text{CH}_4(\text{xs})$ in our samples. Our NGRIP samples
910 reveal a $\delta^{13}\text{C}-\text{CH}_4(\text{xs})$ value (Keeling y-intercept weighted mean) of $(-47.0 \pm 2.9) \text{‰}$ which is
911 within the error consistent with contemporaneous atmospheric values or with emissions from
912 seeping reservoirs of natural gas. In contrast, our $\delta\text{D}-\text{CH}_4(\text{xs})$ measurements on NGRIP samples
913 reveal a very light value (Keeling y-intercept weighted mean) of $(-326 \pm 57) \text{‰}$ and slightly
914 outside of the field of a thermogenic origin (see Fig. 11). The value is similar to the estimate
915 by Lee et al. (2020), which, however, lies inside the field of a thermogenic origin (see Fig. 11).
916 While both the low $\text{CH}_4/(\text{C}_2\text{H}_6+\text{C}_3\text{H}_8)$ ratio and the $\delta^{13}\text{C}-\text{CH}_4(\text{xs})$ could be indicative of a
917 thermogenic source (A1), the light $\delta\text{D}-\text{CH}_4(\text{xs})$ signature is far away from the atmospheric $\delta\text{D}-$
918 CH_4 value and is borderline in line with typical $\delta\text{D}-\text{CH}_4$ values of a thermogenic origin. Hence,
919 our $\delta\text{D}-\text{CH}_4(\text{xs})$ values exclude the atmospheric adsorption scenario A2 and put a question mark
920 after the seep adsorption scenario A1.

hat gelöscht: the

hat gelöscht: evidence

hat gelöscht: hydrogen isotopic

hat gelöscht: $\delta\text{D}-\text{CH}_4(\text{xs})$

922 For the seep adsorption scenario A1 to work the dust particles on which the thermogenic gas
923 adsorbed are not allowed to experience any contact with liquid water prior to the analysis in the

lab. In other words, if the particles get in contact with liquid water after the adsorption step, the adsorbed alkanes would desorb from the particles as they do in the laboratory during melting. Given the occurrence of wet/dry cycles in the source area (Ruth et al., 2007), we question the plausibility of scenario A1. Moreover, we expect the characteristic desorption time to differ between the three alkanes, which would be in contradiction to the observation that the alkane ratios in the 1st and 2nd extraction are the same within the error limits.

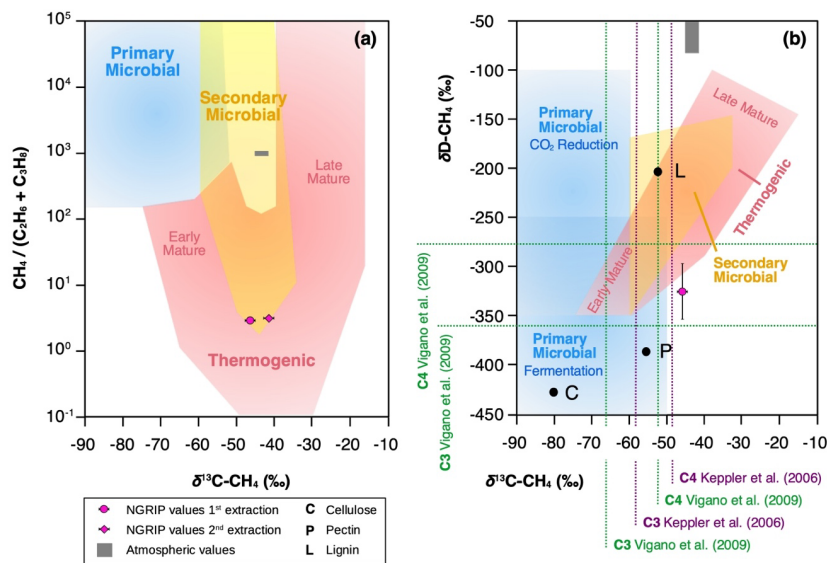


Figure 11: Diagrams of genetic fields for natural gas adopted from Milkov and Etiope (2018). (a) Genetic diagram of $\delta^{13}\text{C-CH}_4$ versus $\text{CH}_4/(\text{C}_2\text{H}_6+\text{C}_3\text{H}_8)$. Typical atmospheric values are indicated by a grey-shaded area, NGRIP values obtained from the 1st and 2nd extraction from this study with a pink dot. (b) Methane genetic diagram of $\delta^{13}\text{C-CH}_4$ versus $\delta\text{D-CH}_4$. Values for cellulose (C), lignin (L) and pectin (P) from Vigano et al. (2009) and mean values for C3 and C4 plants, respectively, from studies by Keppler et al. (2006) and Vigano et al. (2009) are added.

(2) Microbial production

The second process that we take into consideration is the microbial production of excess alkanes through methanogenic microbes. Here we must again differentiate between two scenarios: microbial production can either take place in the ice sheet, (in situ) by extremophile microbes. This process requires that in situ produced excess alkanes are then adsorbed onto dust particles

hat gelöscht: it

Formatiert: Nicht vom nächsten Absatz trennen

hat gelöscht: ¶

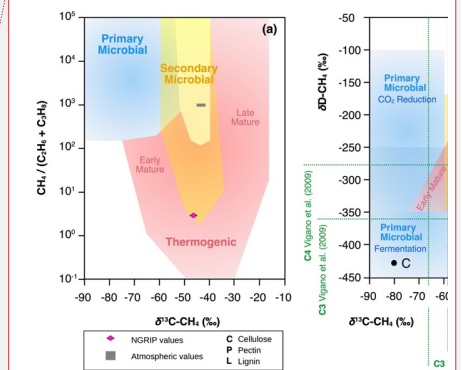


Figure 11: D

hat formatiert: Schriftart: 10 Pt., Schriftfarbe: Text 1

hat formatiert: Schriftart: 10 Pt., Schriftfarbe: Text 1

hat formatiert: Schriftart: 10 Pt., Schriftfarbe: Text 1

hat formatiert: Schriftart: 10 Pt., Nicht Kursiv, Schriftfarbe: Text 1

hat formatiert: Hochgestellt

hat formatiert: Schriftart: 10 Pt., Nicht Kursiv, Schriftfarbe: Text 1

hat gelöscht: a

hat gelöscht: itself

962 in the ice and subsequently slowly desorbed during melting, when in contact with liquid water
 963 (M1). Or the production takes place during the melt extraction when methanogens can
 964 metabolize in liquid water (*in extractu*; M2). Lee et al. (2020) already excluded a “simple” in
 965 situ production of excess CH₄ (microbial in situ production in the ice without an adsorption-
 966 desorption process; M0) and this option will therefore not be further discussed here.

hat gelöscht: extraction

hat gelöscht: methanogenic

hat gelöscht: microbes

967 Our ratios of excess methane/ethane/propane in NGRIP and GRIP samples add another piece
 968 of corroborating evidence that excess alkanes are not produced microbially. The main microbial
 969 production process of methane, the decomposition of organic precursors in an anaerobic
 970 environment by archaea, also co-produces ethane and propane, however only in marginal
 971 amounts. The typical methanogenesis yields >200 times more methane than ethane and propane
 972 (Bernard et al., 1977; Milkov and Etiope, 2018) while we find a molar ratio of methane to
 973 ethane to propane of 14:2:1 in our samples. This renders a microbial production pathway (in
 974 situ and *in extractu*, i.e. M1 and M2) unlikely. Moreover, a microbial production of CH₄ is
 975 unlikely in view of the $\delta^{13}\text{C-CH}_{4(\text{xs})}$ signature which is too heavy for microbial CH₄.

hat gelöscht: ¶

The second part of a potential M1 process, the adsorption of the microbially produced excess alkanes onto dust particles in the ice and the subsequent desorption during melting/extraction, remains difficult to assess. A selective adsorption of the in situ produced alkanes on mineral dust in the ice requires that the in situ production is taking place on the dust particles themselves, which can be questioned but cannot be ruled out. However,

hat gelöscht: o

976 Apart from these quantitative limitations of microbial CH₄ in situ production in ice, there is
 977 evidence from the “microbial inhibition experiment” by Lee et al. (2020) against microbial
 978 production of alkanes during the melt extraction. Lee et al. (2020) tested whether biological
 979 CH_{4(xs)} production in the meltwater was inhibited when the ice core samples were treated with
 980 HgCl₂. As CH_{4(xs)} was still observed in the poisoned samples and as it seems unlikely that
 981 microbes are resistant to HgCl₂, this experiment questions the hypothesis of microbially
 982 produced CH_{4(xs)} also during extraction (*in extractu*).
 983
 984

hat gelöscht: Similar to our argument made for the pure desorption hypothesis, the constant excess alkane ratio in the second and first extraction is difficult to reconcile with an expected different desorption lifetime for the three alkanes. ¶

hat gelöscht: contradicting

hat gelöscht: also for

hat gelöscht: quite

985 We conclude that regardless of the location of the production, in situ or *in extractu*, the
 986 fingerprint of the excess alkanes in our samples (heavy $\delta^{13}\text{C-CH}_{4(\text{xs})}$ signature and low
 987 CH₄/(C₂H₆+C₃H₈) ratio) essentially rules out a microbial source and another (abiotic?) process
 988 for excess alkane production is likely to exist.
 989

hat gelöscht: pathway

hat gelöscht: produced

990 (3) Abiotic/ chemical production

991 In this last section we consider an abiotic or chemical process to be responsible for the observed
 992 excess alkanes, where excess alkanes would be produced through the abiotic decomposition of
 993 labile organic compounds in the meltwater (C2). We question an abiotic in situ production in
 994 the ice (C1) as it would require the quantitative adsorption of the in situ produced alkanes onto
 995 mineral dust particles but not the atmospheric CH₄ that is available in the ice otherwise.

hat gelöscht: Based on the same arguments presented in the previous section for a microbial in situ production, we also

1020 However, as the location of an in situ excess CH₄ production in the ice is not the same as the
1021 location of the bubble or clathrates in the ice, this argument is not able to exclude this
1022 hypothesis. However, given the age of the ice that allows for permeation of gases on the grain
1023 scale and the recrystallization of the ice during that time, which both could bring the
1024 atmospheric CH₄ in contact with the dust particles, we feel this process is less plausible than a
1025 potential C2 mechanism. Moreover (as mentioned before), in view of the expected different
1026 desorption characteristics of the three alkanes, we would expect different alkane ratios in the
1027 1st and 2nd extraction, which is not the case. Accordingly, a direct abiotic production during
1028 melting appears to be more likely than a desorption process.

hat gelöscht: the

hat gelöscht: process

1029
1030 Organic precursors for this abiotic production during extraction could be any organic matter
1031 (either microbial or plant-derived). As the amount of excess alkanes is tightly coupled to the
1032 amount of dust, we assume that these organic compounds are attached to dust particles. This
1033 “docking” of the organic precursor onto the mineral dust could happen already in the dust
1034 source region involving organic material available at the surface. Or it could happen by
1035 adhering of volatile organic molecules or secondary organic aerosols from the atmosphere to
1036 the mineral dust aerosol either before deflation at the source region or during transport to
1037 Greenland.

1038
1039 We consider this pathway plausible, as in recent years the prevailing paradigm that methane is
1040 only produced by methanogenic archaea under strictly anaerobic conditions has been
1041 challenged. Several experimental studies demonstrated that methane can also be released from
1042 dried soils (Hurkuck et al., 2012; Jugold et al., 2012; Wang et al., 2013; Gu et al., 2016), fresh
1043 plant matter and dry leaf litter (Keppler et al., 2006; Vigano et al., 2008, 2009, 2010; Bruhn et
1044 al., 2009; Derendorp et al., 2010, 2011), different kinds of living eukaryotes (plants, animals
1045 and fungi) (Liu et al., 2015), single organic structural components (McLeod et al., 2008;
1046 Messenger et al., 2009; Althoff et al., 2014) and in fact under aerobic conditions. Most of these
1047 studies focused on methane, however, there is also evidence for simultaneous formation of other
1048 short-chain hydrocarbons like ethane and propane (McLeod et al., 2008; Derendorp et al., 2010,
1049 2011). At least three mechanisms have been identified to be relevant: i) photo-degradation, ii)
1050 thermal degradation, or iii) degradation by the reaction with a reactive oxygen species (ROS)
1051 (Schade et al., 1999; Wang et al., 2017). Common to all three pathways is a functional group
1052 (for example a methyl or ethyl group) that is cleaved from the organic precursor molecule. Key
1053 parameters that control the production of abiotic methane are mainly temperature, UV radiation,

1056 water/ moisture, and the type of organic precursor material (Vigano et al., 2008; Derendorp et
1057 al., 2010, 2011; Hurkuck et al., 2012; Jugold et al., 2012; Wang et al., 2013, 2017).

1058

1059 Recent findings demonstrated the large variety of potential organic precursors for abiotic trace
1060 gas formation. For methane formation, the plant structural components pectin and lignin have
1061 been identified in many studies as a precursor in different plant materials. Pectin and lignin
1062 contain methoxyl-groups in two different chemical types, ester methoxyl (present in pectin) and
1063 ether methoxyl (present in lignin) (Keppler et al., 2006, 2008; McLeod et al., 2008; Messenger
1064 et al., 2009; Bruhn et al., 2009; Vigano et al., 2008; Hurkuck et al., 2012; Liu et al., 2015; Wang
1065 et al., 2017). Ester methyl groups of pectin were also discovered as precursor for ethane
1066 formation (McLeod et al., 2008). Overall, pectin makes up a large fraction of the primary cell
1067 wall mass of many plants, thus, representing a large reservoir available as precursor for abiotic
1068 alkane formation (Keppler et al., 2006; Mohnen et al., 2008; Vigano et al., 2008, 2010; McLeod
1069 et al., 2008), and may be present in sufficient quantities in our ice core samples attached to
1070 mineral dust particles. CH₄ production was also detected from cellulose even though it does not
1071 contain methoxyl groups suggesting that other carbon moieties of polysaccharides might allow
1072 abiotic CH₄ formation (Keppler et al., 2006; Vigano et al., 2008). In addition, poly-unsaturated
1073 fatty acids in plant membranes are suggested to play a key role not only in the formation of
1074 methane but also for ethane and propane (John and Curtis, 1977; Dumelin and Tappel, 1977;
1075 Derendorp et al., 2010, 2011). Further, sulfur-bound methyl groups of methionine are an
1076 important precursor for abiotic CH₄ formation in fungi (Althoff et al., 2014).

1077

1078 Considerably different emission rates were found for the same amount but different type of
1079 organic substances leading to the conclusion that abiotic emissions are strongly dependent on
1080 the type of organic precursor material or single structural components (Keppler et al., 2006;
1081 McLeod et al., 2008; Vigano et al., 2008; Messenger et al., 2009; Hurkuck et al., 2012). Other
1082 factors such as leaf and cell wall structure (McLeod and Newsham, 2007; Watanabe et al.,
1083 2012; Liu et al., 2015) and the organic carbon content (Hurkuck et al., 2012) are suggested to
1084 influence this process, too.

1085

1086 To explain the observed excess alkanes in dust-rich Greenland ice core samples by an abiotic
1087 production through the decomposition of labile organic compounds requires adequate quantities
1088 of organic precursors within the ice core samples. Certainly, such material is present in
1089 Greenland ice, but currently, there is no record on the amount and type of organic substances

hat gelöscht: the formation of methane

hat gelöscht: organic

hat gelöscht: have an important

hat gelöscht: s

hat gelöscht: on

hat gelöscht: to be present

1096 available. We have some limited information from occasional Greenland ice core samples in
1097 which different types of organic substances were detected (Giorio et al., 2018, and references
1098 therein), but it does not allow for an overarching interpretation for our ice samples. A NGRIP
1099 record on formaldehyde and a GRIP record on acetate and formate exists (Fuhrer et al., 1997),
1100 which suggest lower levels during the glacial, but as we do not know which organic precursors
1101 lead to the excess CH₄ productions this observation is only of limited value.

hat gelöscht: in NGRIP and GRIP ice

1102
1103 We may also question whether a perfect record of eligible precursor molecules could exist at
1104 all. As we observe that precursor substances are labile and quickly decompose when in contact
1105 with liquid water, a direct measurement of these substances might not be possible but only for
1106 similar, non-reactive substances, which are then not qualified as precursors for the reaction
1107 observed. The problems of sampling, analysis and interpretation of organic material in polar
1108 ice are well summarized and expounded in Giorio et al. (2018).

1109
1110 In any case, it appears likely that the mineral dust carries along soil organic matter or plant
1111 residues or accumulates organic aerosols as a result of organic aerosol aging during transport.
1112 In our data we see a relationship between the amount of mineral dust within the ice core samples
1113 and the amount of excess alkanes. As the amount of excess alkanes per Ca²⁺ (or mass of dust)
1114 is variable, this suggests that mineral dust is just a carrier for (a variable amount of) organic
1115 substances but does not account for the production of excess alkanes itself. The dust content
1116 within the ice core sample can only serve as a rough estimate of organic precursor availability
1117 and whether an abiotic production from organic precursor substances is likely to occur during
1118 extraction.

hat gelöscht: therefore

1119
1120 Again, our experiments can shed some light on the viability of this pathway for excess alkane
1121 production. If we assume that the dust-related organic matter in the ice represents a reservoir
1122 available for abiotic production, then the decomposition continues until all functional groups
1123 are cleaved from their organic precursor molecules and released as excess alkanes. Once the
1124 reservoir is emptied, excess alkane production ceases (Derendorp et al., 2010, 2011). In line,
1125 we interpret that the decrease in the amount of measured excess alkanes from the 1st to the 2nd
1126 extraction may result from an exhaustion of the precursor reservoir. The reaction time is slow
1127 enough to allow for the continuing production during the second extraction but too slow for a
1128 detectable production during continuous flow analysis of CH₄, where the water phase is present
1129 only for less than two minutes before gas extraction. The significantly reduced production

hat gelöscht: an

1133 during the 2nd extraction in our samples shows that the time scale for this process is hours (see
1134 Fig. C1) until the reservoir of functional groups is depleted. We note that this implies that the
1135 amount of excess alkanes is strongly dependent on the time span when liquid water is in contact
1136 with the dust, which varies among the methods used for CH₄ analyses. Thus, any excess CH₄
1137 in measurements from different labs performed under different conditions may differ.

1138

1139 To explain an abiotic alkane production, certain conducive boundary conditions must be met.
1140 The most important parameters that control non-microbial trace gas formation are temperature
1141 and UV radiation. This was demonstrated in many field and laboratory experiments (Keppler
1142 et al., 2006; McLeod et al., 2008; Vigano et al., 2008, 2009; Messenger et al., 2009; Bruhn et
1143 al., 2009; Derendorp et al., 2010, 2011; Hurkuck et al., 2012; Jugold et al., 2012; Wang et al.,
1144 2017). Generally, increasing temperatures lead to exponentially increasing CH₄ emissions
1145 (Vigano et al., 2008; Bruhn et al., 2009; Wang et al., 2013; Liu et al., 2015). The same behaviour
1146 was observed for ethane and propane with very low emissions at ambient temperatures (20-
1147 30°C) and a maximum at 70°C (McLeod et al., 2008; Derendorp et al., 2010, 2011). At constant
1148 temperatures emission rates decreased over time, which is at high temperatures on the timescale
1149 of hours and at ambient temperatures of months. Even after months, some production was
1150 observed, pointing to a slowly depleting reservoir of organic precursors (Derendorp et al., 2010,
1151 2011). Increasing emissions observed at temperatures >40°C were also used as indicator to
1152 exclude the possibility of enzymatic activity, as the denaturation of enzymes would lead to
1153 rapidly declining emissions at higher temperatures (Keppler et al., 2006; Derendorp et al., 2011;
1154 Liu et al., 2015). We note that our sample extraction takes place at 0°C or a few °C above,
1155 hence, temperature conditions during the extraction are not conducive of the type of abiotic
1156 alkane production as observed in the studies listed above. Whether the cool temperature of the
1157 meltwater during extraction inhibits abiotic reaction is difficult to say. Derendorp et al. (2010,
1158 2011) observed a much lower temperature dependency of C2-C5 hydrocarbon emissions from
1159 ground leaves than whole leaves, which might also apply to our samples with very fine
1160 fragments of organic substances attached to dust particles.

1161

1162 Besides the strong relationship to temperature also UV irradiation seems to have a substantial
1163 effect on abiotic production. Studies on irradiated samples (dry and fresh plant matter, plant
1164 structural components) showed a linear increase in methane emissions, while UV-B irradiation
1165 seems to have a much stronger effect on the release compared to UV-A (Vigano et al., 2008;
1166 McLeod et al., 2008; Bruhn et al., 2009; Jugold et al., 2012). The influence of visible light (400-

hat gelöscht: an

1168 700 nm), however, seems controversial (Keppler et al., 2006; Bruhn et al., 2009; Austin et al.,
1169 2016). Further, samples that were heated and irradiated show a different emission curve than
1170 just heated samples, indicating that irradiation changes the temperature dependency, in turn
1171 pointing to the fact that different chemical pathways exist (Vigano et al., 2008).

1172 In dark experiments on plant material at different temperatures CH₄ emissions were still
1173 observed, while again higher temperatures revealed much higher emissions, emphasizing the
1174 strong temperature dependency also without UV irradiation (Vigano et al., 2008; Wang et al.,
1175 2008; Bruhn et al., 2009). The release of ethane along with methane from pectin was also
1176 stimulated under UV radiation (McLeod et al., 2008).

1177
1178 Regarding our measurements, the sample vessel in the $\delta^{13}\text{C}$ -CH₄ device is encased by a UV
1179 blocker foil absorbing the shortwave (<600 nm) emissions from the heating bulbs when melting
1180 the ice sample, while in the δD -CH₄ device, the sample vessel is completely shielded from light
1181 (Sect. 2.2 and 2.3). Two NGRIP ice core samples were measured with the $\delta^{13}\text{C}$ -CH₄ device in
1182 the dark (“dark extraction”) showing the same amount of excess alkanes as the regular
1183 measurements at day light. This indicates that light >600 nm has no influence on an *in extractu*
1184 reaction during our measurements.

1185
1186 We stress that although we can exclude a direct UV effect during melting, it is possible that UV
1187 irradiation during dust aerosol transport to Greenland and within the upper snow layer after
1188 deposition until the snow gets buried into deeper layers may precondition organic precursors
1189 attached to dust to allow for alkane production to occur during the melt extraction. In particular,
1190 the first step of the reaction (excitation of the homolytic bond of a precursor compound) may
1191 start already in the atmosphere or in the snow, where UV radiation is available. Within the ice
1192 sheet the reaction may be paused (“frozen reaction”) and the total reaction pathway is only
1193 completed during the melting process when liquid water is present.

1194
1195 Finally, we consider the role of reactive oxygen species in an abiotic production pathway. ROS
1196 are widely produced in metabolic pathways during biological activity but also during
1197 photochemical reactions with mineral oxides (Apel and Hirt, 2004; Messenger et al., 2009;
1198 Georgiou et al., 2015). Through their high oxidative potential, ROS can cleave functional
1199 groups from precursor compounds. Several studies have demonstrated this mechanism for the
1200 production of abiotic CH₄ in soils and plant matter (McLeod et al., 2008; Messenger et al.,
1201 2009; Althoff et al., 2010, 2014; Jugold et al., 2012; Wang et al., 2011, 2013) and for other
1202 trace gases such as CO₂, ethane, and ethylene from plant pectins (McLeod et al., 2008). UV

hat gelöscht: sample extraction

hat gelöscht: mineral

hat gelöscht: upper firm layer

hat gelöscht: energy from

hat gelöscht: are capable to

1208 radiation or thermal energy has no direct influence on the degradation process by the reaction
1209 with ROS, however, it might also be a stimulating factor and evoke further indirect reactions.
1210 For instance, UV radiation can lead to changes in plants which in turn lead to ROS generation
1211 (Liu et al., 2015). It was demonstrated that UV radiation induces the formation of organic
1212 photosensitizers or photo-catalysts which increase CH₄ emissions from pectin (Messenger et
1213 al., 2009) and clay minerals. For example, the formation of hydroxyl radicals from
1214 montmorillonite and other clay minerals upon UV (and visible light) irradiation shows that
1215 clays might play a significant role in the oxidation of organic compounds on their surface
1216 (Katagi, 1990; Wu et al., 2008; Kibanova et al., 2011).

hat gelöscht: OH

hat gelöscht: in different environments

1218 It has been proven that the species type and the overall amount of ROS available for, or involved
1219 in a reaction, has a significant effect on the amount of emissions through such a process (Jugold
1220 et al., 2012; Wang et al., 2013, 2017). For the production of methane (and ethane), hydrogen
1221 peroxide (H₂O₂) and hydroxyl radicals have been proven to be the prominent species
1222 (Messenger et al., 2009; Althoff et al., 2010; Wang et al., 2011, 2013; Jugold et al., 2012;
1223 McLeod et al., 2008). Such ROS could be already present in the snow and ice or being produced
1224 in the meltwater. For example, H₂O₂ can be unambiguously detected in Greenland Holocene
1225 ice using CFA, however, H₂O₂ in dusty glacial ice is mostly below the detection limit, likely
1226 due to oxidation reactions in the ice sheet or during melt extraction.

hat gelöscht: (OH

hat gelöscht:)

1228 In summary, we believe that in our case of excess alkane production/ release in the meltwater
1229 at low temperatures and without any UV irradiation, the ROS-induced mechanism appears
1230 possible. In experiments with plant pectin McLeod et al. (2008) observed not only CH₄ but also
1231 ethane and found a methane to ethane production ratio of around 5 which is similar to our value
1232 of around 7. Accordingly, we see that a ROS-induced production pathway has the potential to
1233 explain excess alkanes in our samples, however, little is known about ROS chemistry in ice in
1234 particular for reactions with organic precursors and more research is needed to understand the
1235 role of ROS in organic decomposition in ice. Another alternative to the two-stage reaction
1236 pathway with ROS would be a reaction catalyzed in the meltwater by dust-derived transition
1237 metals. This has been observed for example for the oxidation of SO₂ in water-activated aerosol
1238 particles (Harris et al., 2013), but to our knowledge it has not been described in the literature
1239 for alkane production via organic precursors so far. Accordingly, we can only speculate on this
1240 pathway at the moment.

hat gelöscht: cores

1247
1248
1249
1250
1251
1252
1253
1254
1255
1256
1257
1258
1259
1260
1261
1262
1263
1264
1265
1266
1267
1268
1269
1270
1271
1272
1273
1274
1275
1276
1277
1278
1279
1280
1281
1282
1283
1284
1285
1286
1287

Another key parameter influencing all abiotic pathways might be the presence of liquid water or moisture. In experiments testing the hypothesis of non-microbial CH₄ formation in different soil samples, it was demonstrated that adding water/moisture led to an up to eight-fold increase in CH₄ emissions (Hurkuck et al., 2012; Jugold et al., 2012; Wang et al., 2013). It is hypothesized that the presence of liquid water or moisture stimulates (in addition to heating or UV radiation) the cleaving process of a functional group from the primary precursor and therefore increases the production of CH₄. With respect to our observations on NGRIP and GRIP samples the presence of water seems to be a fundamental parameter influencing the second step of a “frozen reaction” *in extractu* process, where the duration of water presence plays an important role.

A final puzzle piece for a possible abiotic methane production comes from our dual isotopic fingerprints of the excess CH₄. As illustrated in Fig. 11 (right panel) our $\delta D-CH_{4(xs)}$ signature lies well within the distribution of the hydrogen isotopic composition of CH₄ produced from potential organic precursors. For $\delta^{13}C$ our values lie outside and on the heavier side of the carbon isotope signature spectrum.

We conclude that despite our inability to pinpoint the exact organic precursors that lead to abiotic excess alkane production during the melt extraction of our ice samples, both the ratio of the excess alkanes as well as the isotopic signature of excess CH₄ is generally in line with this pathway. Thus, without further contradicting evidence from targeted studies on organic precursors in ice core samples and their chemical degradation, we believe that the ROS-induced production pathway is to date the most likely explanation for the observed excess alkanes during extraction. However, we cannot completely rule out an adsorption-desorption process of thermogenic gas on dust particles.

hat gelöscht: the addition of

hat gelöscht: compound

hat gelöscht: . However, it seems that the stimulating effect by of water cannot be generalized, as Wang et al. (2013) emphasized that this process is highly dependent on “water of proper amount”. In their experiments, CH₄ emissions from peat and grassland soil samples treated with a varying amount of water in oxic–anoxic cycles at 70°C were measured. They observed that under both aerobic and anaerobic conditions water does not always stimulate non-microbial CH₄ release and that too much water can also suppress CH₄ emissions. Wang et al. (2013) observed differences between different soil samples in response to a varying water content indicating that the water effect is different for different precursors.

hat gelöscht: isotopic

hat gelöscht: at this point

Table 1: Overview of the different hypotheses explaining the possible sources for excess alkanes (as illustrated in Figure 10) in relation to our experimental observations. A green checkmark indicates that the observation is in line with the respective mechanism, a black cross indicates that the observation is in not line with the respective mechanism. A grey shaded area means that this observation does not apply or does not affect the respective mechanism.

1309

	(1) ADSORPTION- DESORPTION OF THERMOGENIC/ ATMOSPHERIC GAS		(2) MICROBIAL PRODUCTION			(3) ABIOTIC/ CHEMICAL PRODUCTION	
	A1	A2	M0	M1	M2	C1	C2
Correlation to Ca ²⁺ / mineral dust	✓	✓	✓	✓	✓	✓	✓
Alkane pattern	✓	✗	✗	✗	✗	(✓)	(✓)
CFA evidence			✗				
δ ¹³ C-CH _{4(xs)}	✗	✓	✗	✗	✗	(✓)	(✓)
δD-CH _{4(xs)}	✓	✗	✓	✓	✓	(✓)	(✓)
δD-CH _{4(xs)} estimated by Lee et al. (2020)	✓	✗	✓	✓	✓	(✓)	(✓)
Poisoning experiment by Lee et al. (2020)					✗		

1310

1311

5. Conclusions and Outlook

1313

The comparison of methane records from ice cores samples measured with different melt extraction techniques requires careful consideration and interpretation. Non-atmospheric methane contributions to the total methane concentration were discovered in specific Greenland ice core sections pointing to a process occurring during the wet extraction. To better assess this finding, we measured new records of [methane], [ethane], [propane], δD-CH₄, and δ¹³C-CH₄ on discrete NGRIP and GRIP ice core samples using two different wet extraction systems. With our new data we confirm the production of CH_{4(xs)} in the meltwater and quantify its dual isotopic signature. With the simultaneous detection of ethane and propane we discovered that these short-chain alkanes are co-produced in a fixed molar ratio pointing to a common production pathway. With our 2nd extraction we constrained the temporal dynamics of this process, which occurs on the timescale of hours.

1325

1327 Based on our new experimental data we provide an improved assessment of potential
 1328 mechanisms that could explain the observed variations in NGRIP and GRIP ice samples. A
 1329 microbial CH₄ production represents an obvious candidate, but regardless of whether this CH₄
 1330 is produced in situ or *in extractu*, several lines of evidence gained from our measurements (low
 1331 CH₄/(C₂H₆+C₃H₈) ratio, heavy $\delta^{13}\text{C}$ -CH_{4(x)s} signature) demonstrate that the fingerprint of the
 1332 produced excess alkanes is unlikely of microbial origin. Also an adsorption-desorption process
 1333 of atmospheric or thermogenic CH₄ on dust particles does not match many of our observations
 1334 and is therefore unlikely. However, with the current knowledge we cannot definitely exclude
 1335 such an adsorption of thermogenic gas to be responsible for the observed excess alkane levels
 1336 in our samples.

1337

1338 At present we favor to explain the formation of excess alkanes by abiotic decomposition of
 1339 organic precursors during prolonged wet extraction. Such an abiotic source for methane and
 1340 other short-chain alkanes was discovered previously in other studies (Keppler et al., 2006;
 1341 Vigano et al., 2008, 2009, 2010; Messenger et al., 2009; Hurkuck et al., 2012; Wang et al.,
 1342 2013, and others listed above) using different organic samples, e.g. from plant or soil material,
 1343 however, this process has not been connected to excess CH₄ production during ice core
 1344 analyses. This process matches many of our observations, and such a mechanism can be
 1345 responsible for excess alkanes in Greenland ice core samples. To better assess a potential abiotic
 1346 production process in ice analyses the most important questions to solve in the future are: What
 1347 are the specific precursor substances? Which parameters control an abiotic production during
 1348 wet extractions? How does the fixed molar ratio between methane, ethane, and propane come
 1349 about in this process? And finally, in which way is this excess alkane production causally
 1350 related to the amount of mineral dust within the ice sample?

1351

1352 Identifying a specific reaction pathway that leads to the short-chain alkanes with their observed
 1353 ratios would certainly benefit from identifying targeted organic precursor substances in the ice.
 1354 However, detecting these postulated organic precursors in the ice core is inherently difficult as
 1355 these compounds are very labile in water as our experiments demonstrated that after about 30
 1356 min only a fraction of these compounds remains in the meltwater while the majority already
 1357 reacted to excess alkanes. Future studies may also focus on further isotope measurements ($\delta^{13}\text{C}$ -
 1358 CH₄ and δD -CH₄) including isotope labeling experiments providing an option to
 1359 unambiguously detect methane produced during the measurement procedure in a commonly

hat gelöscht: several

hat gelöscht:

hat gelöscht: be relevant for

hat gelöscht: in principle

hat gelöscht: to have a

hat gelöscht: source

hat gelöscht: must be

hat gelöscht: ic

1368 used wet extraction technique, and again, to uncover potential reaction mechanisms for CH_{4(xs)}
1369 production.

1370

1371 To better assess the viability of the alternative hypothesis of a release of previously adsorbed
1372 alkanes from dust particles (scenario A1 and A2) during the extraction, dust particles from the
1373 Taklamakan or Gobi desert need to be tested whether they contain relevant amounts of adsorbed
1374 alkanes that are released when in contact with liquid water. A second step could be to expose
1375 such dust samples to high levels of alkanes to mimic the adsorption process of natural gas seeps.
1376 It also needs to be shown that the adsorbed alkanes stay adsorbed on the dust particles for a
1377 prolonged time (months, ideally years) after exposing the particles to ambient air and that
1378 droplet and ice nucleation during aerosol transport does not lead to a loss of the previously
1379 adsorbed CH₄. To quantify any isotopic fractionation involved with the ad- and desorption step,
1380 $\delta^{13}\text{C-CH}_4$ and $\delta\text{D-CH}_4$ analyses will be most valuable.

1381

1382 Finally, our studies clearly show that the published Greenland ice core CH₄ record is biased
1383 high for selected (glacial, dust-rich) time intervals and needs to be corrected for the excess CH₄
1384 contribution. This is particularly important for studies of the IPD in CH₄ and stable isotope
1385 ratios of methane. Methodological ways to remedy excess methane (and ethane and propane)
1386 in future measurements of atmospheric [CH₄] from air trapped in ice cores could be to use
1387 continuous online CH₄ measurements, which apparently avoid sizeable CH_{4(xs)} production. But
1388 also dry extraction methods and sublimation techniques for discrete samples, which are
1389 expected to avoid *in extractu* production by evading the melting phase, could be used. Finally,
1390 our own $\delta^{13}\text{C-CH}_4$ device, which allows to measure $\delta^{13}\text{C-CH}_4$ as well as methane, ethane, and
1391 propane concentrations from the same sample, can be used to correct the measured CH₄ values
1392 making use of the co-production of the other two alkanes.

1393

1394 CH_{4(xs)} needs to be corrected for when interpreting the already existing discrete CH₄ records
1395 and its stable isotopes in dust-rich intervals in Greenland ice core samples. Impact of CH_{4(xs)} on
1396 interpreting past atmospheric [CH₄] will only slightly affect radiative forcing reconstructions,
1397 however, it will have a significant effect on the assessment of the global CH₄ cycle and in
1398 particular on the hemispheric CH₄ source distribution which is based on the IPD. We observe
1399 that in some intervals, CH_{4(xs)} is in the same range as the previously reconstructed IPD implying
1400 that correcting for CH_{4(xs)} will lower the IPD considerably and hence lower also the relative
1401 contribution of northern hemispheric sources at those times. We see that there is an urgent need

hat gelöscht: It is clear that

hat gelöscht: the

1404 to reliably revisit Greenland ice core CH₄ records for the excess CH₄ contribution. In future
1405 work we aim to establish an applicable correction for excess methane (CH_{4(xs)}, δ¹³C-CH_{4(xs)},
1406 δD-CH_{4(xs)}) in existing records using the co-production ratios of methane, ethane, and propane,
1407 the isotop~~e~~ mass balance of excess and atmospheric CH₄ in ice core samples as well as the
1408 overall correlation of excess CH₄ with the mineral dust content in the ice.

hat gelöscht: and in

hat gelöscht: eic

1440 **Appendix A**
1441

1442
1443
1444
1445
1446
1447
1448
1449

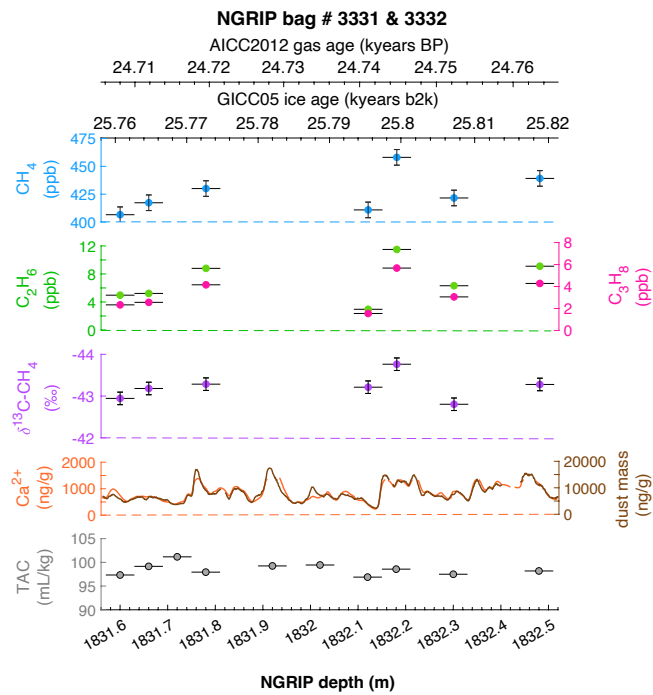


Figure A1: **Detailed data overview for the neighbouring NGRIP bags 3331 & 3332.** Bag-specific overview of several parameters measured for each sample in this bag: methane, ethane, propane, Ca²⁺, mineral dust mass, TAC (Total Air Content), $\delta^{13}\text{C-CH}_4$, indicated at the NGRIP depth (bottom axis) and the AICC2012 gas age (upper top axis) and the GIACC05 ice age (lower top axis). The mineral dust record is taken from Ruth et al. (2003), the Ca²⁺ record from Erhardt et al. (2022).

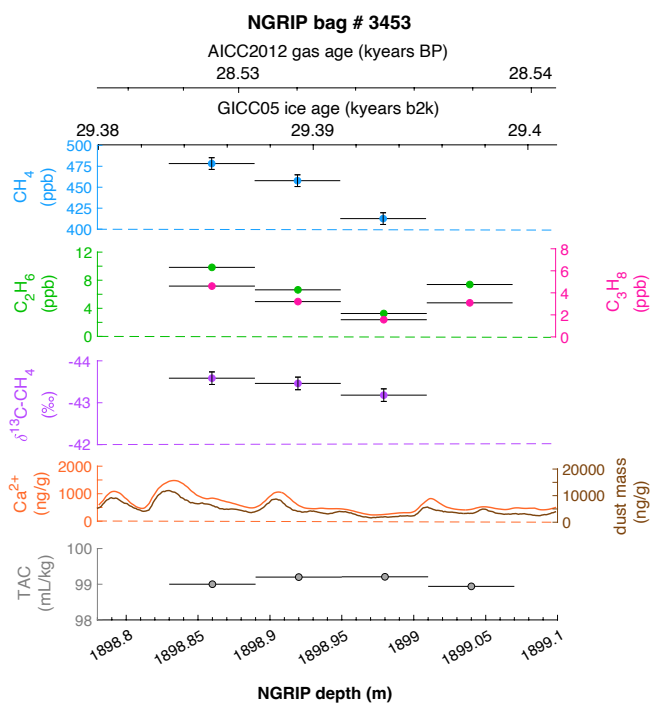


Figure A2: **Detailed data overview for NGRIP bag 3453.** Bag-specific overview of parameters measured for each sample in this bag: methane, ethane, propane, Ca^{2+} , mineral dust mass, TAC (Total Air Content), $\delta^{13}\text{C-CH}_4$, indicated at the NGRIP depth (bottom axis) and the AICC2012 gas age (upper top axis) and the GICC05 ice age (lower top axis). The mineral dust record is taken from Ruth et al. (2003), the Ca^{2+} record from Erhardt et al. (2022).

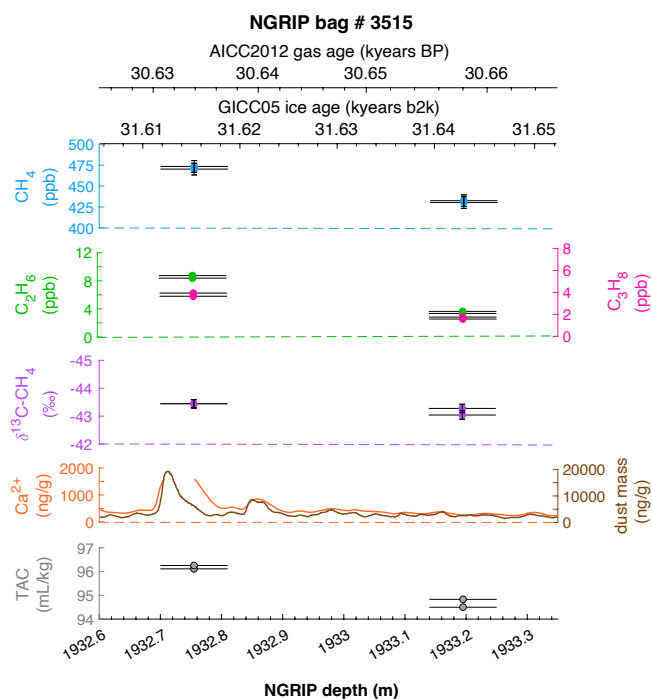


Figure A3: **Detailed data overview for NGRIP bag 3515.** Bag-specific overview of parameters measured for each sample in this bag: methane, ethane, propane, Ca²⁺, mineral dust mass, TAC (Total Air Content), δ¹³C-CH₄, indicated at the NGRIP depth (bottom axis) and the AICC2012 gas age (upper top axis) and the GICC05 ice age (lower top axis). The mineral dust record is taken from Ruth et al. (2003), the Ca²⁺ record from Erhardt et al. (2022). Note that there is a gap in the Ca²⁺ record which was corrected by a fill routine for the analysis of the two measured samples at this depth.

Appendix B

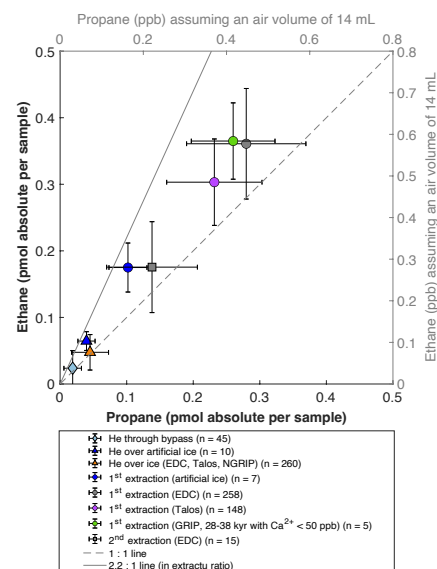


Figure B1: Collection of different measurement modes and ice core sample locations to estimate individual blank contributions. The mode “He through bypass” (diamond) refers to a measurement type where helium is injected into our system but without flowing through our extraction vessel. “He over ice” (triangles) refers to helium injections over the unmelted ice core sample. Results from the 1st extraction are shown for different ice cores (artificial gas-free ice, Talos Dome, EDC, GRIP; colored circles). The 2nd extraction of the Antarctic EDC ice core is marked as grey square. Lines with ethane/propane ratios are for orientation only.

In this section we provide background information of how we determined the blank contributions for our alkane measurements for the different measurement modes. Overall, our strategy is similar to the measurements which were published earlier in 2014 (Schmitt et al., 2014). Here we include more measurements performed since then with our $\delta^{13}\text{C}-\text{CH}_4$ device. Following the classic usage, blank contributions are related to the measurement device itself rather than to the sample, thus we report the measured values of the species as absolute amount in pmol with respect to a measurement procedure (sample run). To compare these absolute values with the classic units of species concentration in the air for an ice sample in ppb, Fig. B1 has secondary axes (grey) for the species concentrations in ppb for an assumed sample size of air of 14 mL STP (our typical ice core sample size).

Since our extraction device is at vacuum conditions, a blank contribution from leaks that allow ambient air with relatively high ethane and propane concentrations to be collected together with our sample seems the most straightforward risk. To quantify this leak contribution, we routinely

1505 perform so called “He over ice” runs where a helium flow is passed over the unmelted ice core
1506 sample and the species are trapped on the cold activated carbon trap (see details in Schmitt et
1507 al., 2014). The trapping duration is the same as for the 1st extraction, thus this “He over ice”
1508 run mimics the contribution for the 1st extraction. As can be seen in Fig. B1, for ethane this
1509 “leak contribution” is typically <0.1 ppb, thus small compared to concentrations we see for
1510 dust-rich Greenland ice samples with about 6 ppb (see Fig. 5). However, this “He over ice”
1511 does not capture the actual melting process of the ice sample and represents the lowest blank
1512 boundary for our ice core samples. To mimic the full procedure an ice core samples experiences,
1513 we run a limited number of artificial gas-free ice samples (blue circles in Fig. B1). The ethane
1514 values obtained for these artificial ice sample is around 0.3 ppb and thus considerably higher
1515 than for the procedure without melting. This indicates that the presence of liquid water may
1516 lead to a desorption or production of alkanes from the inner walls of our extraction vessel.
1517 Alternatively, our artificial ice still contains traces of alkanes. So far, we could not solve this
1518 issue and more experiments are needed. A much larger data set on the upper boundary of the
1519 extraction blank comes from routine measurements of Antarctic ice core samples with the
1520 primary target of stable isotope analyses of CH₄ and N₂O. These Antarctic samples cover glacial
1521 and interglacial time intervals and the measured ethane values are typically around 0.55 ppb.
1522 Since the reconstructed atmospheric background for ethane in Antarctic ice is lower with values
1523 in the range of 0.1 – 0.15 ppb for the late Holocene (Nicewonger et al., 2018), a realistic blank
1524 contribution for our 1st extraction is on the order of 0.4 to 0.5 ppb. An additional constraint
1525 comes from five stadial GRIP samples from the time interval 28-38 kyears (green circle in Fig.
1526 B1) that have very low Ca²⁺ content (< 50 ppb) and thus have likely a negligible contribution
1527 from a dust-related *in extractu* component. The measured ethane concentration from these
1528 GRIP samples is very similar to the Antarctic ice core samples. One possible explanation would
1529 be that the atmospheric ethane concentration during the glacial was similar and low for both
1530 hemispheres. Regardless of the individual contributions, for our considerations of dust-related
1531 *in extractu* production in Greenland ice cores the upper estimate for the sum of atmospheric
1532 background and blank contribution is about 0.55 ppb (about 0.35 pmol) for ethane. Since the
1533 ethane to propane ratio for these non-dust contributions is about 1.5, the corresponding propane
1534 values are lower by that value. Importantly, since the ethane to propane ratio for our dust-related
1535 production is with 2.2 rather similar, its impact on the calculated ethane to propane ratio (e.g.
1536 Fig. 4) is very minor and small within the error estimate. For that reason, we did not correct our
1537 Greenland measurements for any blank contribution and showed the values as measured along
1538 with measurements of Antarctic ice cores samples which serve as first-order blank estimates.

Appendix C

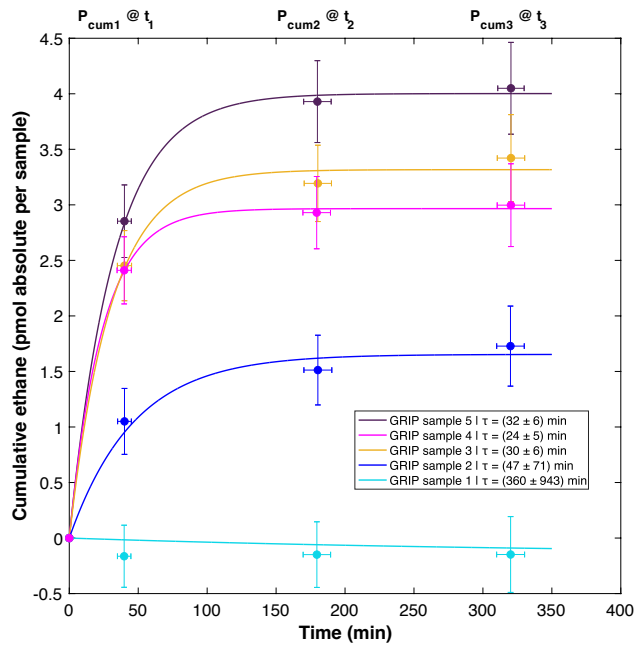


Figure C1: **Temporal dynamics of excess ethane production in GRIP ice core samples.** Cumulative ethane amount from the 1st, 2nd, and 3rd extraction in relation to the time available for a potential reaction in the meltwater during each extraction. We assume a first-order reaction kinetic as model for our observations where the mean half-life time (τ) and standard deviations are calculated for each GRIP sample from the compilation of all 1000 iterations of our Monte Carlo approach. The numbered samples can also be found in Fig. 7a.

The general equation to describe a first-order chemical reaction or exponential decay process (e.g. release of adsorbed gas from the adsorbent) is Eqn. (1).

$$N(t) = N_0 \cdot e^{-(t/\tau)} \quad (1)$$

With N_0 being the total amount of substance (reactant) at the start of the reaction. $N(t)$ equals the remaining amount of the reactant at time t , and t being time of reaction and τ , the mean lifetime of the reaction. In our case, we cannot determine $N(t)$ neither do we know N_0 but we experimentally determined the cumulative amount of the product, $P_{cum(t)}$, at three different times as our observable quantity. Thus, in Eqn. 2 we define $P_{cum(t)}$ as the difference between N_0 and $N(t)$.

1560

1561
$$P_{\text{cum}(t)} = N_0 - N(t) \quad (2)$$

1562

1563 Replacing $N(t)$ in Eqn. 1 with our definition in Eqn. 2 we obtain Eqn. 3, which contains two fit
1564 parameters, N_0 and τ , as well as our observable parameter $P_{\text{cum}(t)}$, i.e. the cumulative amount of
1565 alkane for a certain time step.

1566

1567
$$P_{\text{cum}(t)} = N_0 - N_0 * e(-t/\tau) \quad (3)$$

1568

1569 For the five GRIP samples we have three consecutive measurements each, the 1st, 2nd, and 3rd
1570 extraction. The time-dependent $P_{\text{cum}(t)}$ values are as follows: $P_{\text{cum}0}$ is defined as 0, representing
1571 the state of the unmelted ice sample before liquid water is present. $P_{\text{cum}1}$ is the measured amount
1572 from the 1st extraction (ice extraction) minus the estimated contribution from the atmosphere
1573 and minus the blank contribution for the 1st extraction. $P_{\text{cum}2}$ is the sum of $P_{\text{cum}1}$ and the value
1574 from the 2nd extraction minus the blank contribution of the 2nd extraction. Similarly, $P_{\text{cum}3}$ is the
1575 sum of $P_{\text{cum}2}$ and the value from the 3rd extraction minus the blank for the 3rd extraction.

1576 To account for the uncertainties of the involved measurements and corrections, we added
1577 normally distributed errors to the following parameters (measured value $\pm 5\%$; blank $\pm 20\%$;
1578 atmospheric contribution $\pm 50\%$), and we also assigned an uncertainty of 5 min to the time to
1579 account for variations of the melting speed of the ice and delays between the individual
1580 measurements (1st, 2nd, 3rd).

1581 For the fitting procedure we used the Matlab built in nonlinear least-squares solver called
1582 'lsqcurvefit' and performed 1000 runs where we varied the above-mentioned input parameters.
1583 The output of the function are the two fit parameters, i.e., N_0 and τ . From the 1000 runs we
1584 calculated the mean and the 1 sigma standard deviation of the lifetime.

1585

1586 Note, this approach can only be suitably applied to ethane and propane as the past atmospheric
1587 contribution for these gases in the 1st extraction is typically small against the excess contribution
1588 for dust-rich samples. For our five GRIP samples, where we have three consecutive extractions,
1589 four samples are considered "dust-rich" and are suitable to provide robust estimates for τ . In
1590 contrast, one sample is from an interstadial period with very low dust content and thus shows
1591 negligible production of alkanes in all three extractions. While this sample is not suited to
1592 provide robust estimates for τ , this sample allows to assess the first-order plausibility of the
1593 blank correction and the assumed atmospheric background for ethane for the 1st extraction

hat gelöscht:

1595 (sample number 1, bottom-most sample). For a sample without any *in extractu* production, the
1596 cumulative curve should be flat at around 0 which is the case within our error estimates.

1597

1598

1599

1600 **Code availability**

1601 No special code related to the manuscript.

1602

1603 **Data availability**

1604 Data is provided on request to the authors.

1605

1606 **Author contribution**

1607 The experimental approach was defined by JS, HF and MM. MM and BS performed the
1608 measurements; MM and JS analyzed the data; MM wrote the manuscript draft; MM prepared
1609 the manuscript with contributions from all co-authors.

1610

1611 **Competing interests**

1612 The authors declare that they have no conflict of interest.

1613

1614 **Disclaimer**

1615 None.

1616

1617 **Special issue statement**

1618 Ice core science at the three poles (CP/TC inter-journal SI)

1619

1620 **Acknowledgments**

1621 We thank Murat Aydin for very helpful review comments. The research leading to these results
1622 has received funding from the Swiss National Science Foundation (no. 200020_172506 &
1623 200020B_200328). This work is a contribution to the NorthGRIP ice core project, which is
1624 directed and organized by the Department of Geophysics at the Niels Bohr Institute for
1625 Astronomy, Physics and Geophysics, University of Copenhagen. It is supported by funding
1626 agencies in Denmark (SNF), Belgium (FNRS-CFB), France (IFRTP and NSU/CNRS),
1627 Germany (AWI), Iceland (RannIs), Japan (MEXT), Sweden (SPRS), Switzerland (SNF), and
1628 the United States (NSF).

hat gelöscht: ¶

Formatiert: Block

hat gelöscht: ¶

1659 **References**

- 1660
 1661 Althoff, F., Jugold, A. and Keppler, F.: Methane formation by oxidation of ascorbic acid
 1662 using iron minerals and hydrogen peroxide. *Chemosphere* 80, 286–292,
 1663 <https://doi.org/10.1016/j.chemosphere.2010.04.004>, 2010
 1664
 1665 Althoff, F., Benzing, K., Comba, P., McRoberts, C., Boyd, D. R., Greiner, S. and Keppler, F.:
 1666 Abiotic methanogenesis from organosulphur compounds under ambient conditions, *Nat*
 1667 *Commun*, 5, 4205, <https://doi.org/10.1038/ncomms5205>, 2014
 1668
 1669 Anklin, M., Barnola, J.-M., Schwander, J., Stauffer, B., and Raynaud, D.: Processes affecting
 1670 the CO₂ concentrations measured in Greenland ice, *Tellus*, 47, 461–470,
 1671 <https://doi.org/10.1034/j.1600-0889.47.issue4.6.x>, 1995
 1672
 1673 Apel, K. and Hirt, H.: Reactive Oxygen Species: Metabolism, Oxidative Stress, and Signal
 1674 Transduction, *Annual Review of Plant Biology* 2004, 55:1, 373–399,
 1675 <https://doi.org/10.1146/annurev.arplant.55.031903.141701>, 2004
 1676
 1677 Austin, A. T., Méndez, M. S., and Ballaré, C. L.: Photodegradation alleviates the lignin
 1678 bottleneck for carbon turnover in terrestrial ecosystems, *PNAS*, 13 (16), 4392–4397,
 1679 <https://doi.org/10.1073/pnas.1516157113>, 2016
 1680
 1681 Baumgartner, M., Schilt, A., Eicher, O., Schmitt, J., Schwander, J., Spahni, R., Fischer, H.,
 1682 and Stocker, T. F.: High-resolution interpolator difference of atmospheric methane around the
 1683 Last Glacial Maximum, *Biogeosciences*, 9, 3961–3977, [https://doi.org/10.5194/bg-9-3961-](https://doi.org/10.5194/bg-9-3961-2012)
 1684 2012, 2012
 1685
 1686 Baumgartner, M., Kindler, P., Eicher, O., Floch, G., Schilt, A., Schwander, J., Spahni, R.,
 1687 Capron, E., Chappellaz, J., Leuenberger, M., Fischer, H., and Stocker, T. F.: NGRIP
 1688 CH₄ concentration from 120 to 10 kyr before present and its relation to a $\delta^{15}\text{N}$ temperature
 1689 reconstruction from the same ice core, *Clim. Past*, 10, 903–920, [https://doi.org/10.5194/cp-](https://doi.org/10.5194/cp-10-903-2014)
 1690 10-903-2014, 2014
 1691
 1692 Beck, J., Bock, M., Schmitt, J., Seth, B., Blunier, T., and Fischer, H.: Bipolar carbon and
 1693 hydrogen isotope constraints on the Holocene methane budget, *Biogeosciences*, 15, 7155–
 1694 7175, <https://doi.org/10.5194/bg-15-7155-2018>, 2018
 1695
 1696 Bernard, B., Brooks, J.M. and Sackett, W.M.: A geochemical model for characterization of
 1697 hydrocarbon gas sources in marine sediments. In: 9th Annual Offshore Technology
 1698 Conference, Houston, Texas, May 1977, 435–438 (OTC 2934), [https://doi.org/10.4043/2934-](https://doi.org/10.4043/2934-MS)
 1699 MS, 1977
 1700
 1701 Biscaye, P. E., Grousset, F. E., Revel, M., Van der Gaast, S., Zielinski, G. A., Vaars, A. and
 1702 G. Kukla: Asian provenance of Glacial dust (stage 2) in the Greenland Ice Sheet Project 2 Ice
 1703 Core, Summit, Greenland, *J. Geophys. Res.*, 102, 26,765–26,781, 1997
 1704
 1705 Bock, M., Schmitt, J., Behrens, M., Möller, L., Schneider, R., Sapart, C. and Fischer, H.: A
 1706 gas chromatography/pyrolysis/isotope ratio mass spectrometry system for high- precision dD
 1707 measurements of atmospheric methane extracted from ice cores, *Rapid Commun. Mass*
 1708 *Spectrom*, 24, 621–633, <https://doi.org/10.1002/rcm.4429>, 2010a
 1709

Feldfunktion geändert

hat gelöscht: .,

hat gelöscht: et,

hat gelöscht:

hat gelöscht: l, M.,

hat gelöscht: t, S.,

hat gelöscht: i, G. A.,

hat gelöscht: s, A. and

hat gelöscht: a: As

hat gelöscht: d, J.

hat gelöscht: .,

hat gelöscht: ,

hat gelöscht: –

hat gelöscht: ,

hat formatiert: Schriftart: Nicht Kursiv

1723 Bock, M., Schmitt, J., Blunier, T., Fischer, H., Möller, L. and Spahni, R.: Hydrogen
 1724 Isotopes Preclude Marine Hydrate CH₄ Emissions at the Onset of Dansgaard-Oeschger
 1725 Events, *Science*, 328, 1686-1689, <https://doi.org/10.1126/science.1187651>, 2010b
 1726
 1727 Bock, M., Schmitt, J., Beck, J., Schneider, R., and Fischer, H.: Improving accuracy and
 1728 precision of ice core $\delta D(CH_4)$ analyses using methane pre-pyrolysis and hydrogen post-
 1729 pyrolysis trapping and subsequent chromatographic separation, *Atmos. Meas. Tech.*, 7, 1999–
 1730 2012, <https://doi.org/10.5194/amt-7-1999-2014>, 2014
 1731
 1732 Bock, M., Schmitt, J., Beck, J., Seth, B., Chappellaz, J. and Fischer, H.: Glacial/ interglacial
 1733 wetland, biomass burning, and geologic methane emissions constrained by dual stable
 1734 isotopic CH₄ ice core records, *PNAS*, 114 (29), E5778-E5786,
 1735 <https://doi.org/10.1073/pnas.1613883114>, 2017
 1736
 1737 Bruhn, D., Mikkelsen, T. N., Øbro, J., Willats, W. G. T. and Ambus, P.: Effects of
 1738 temperature, ultraviolet radiation and pectin methyl esterase on aerobic methane release from
 1739 plant material, *Plant Biology*, 11, 43-48, <https://doi.org/10.1111/j.1438-8677.2009.00202.x>,
 1740 2009
 1741
 1742 Campen, R. K., Sowers, T., and Alley, R. B.: Evidence of microbial consortia metabolizing
 1743 within a low-latitude mountain glacier, *Geology*, 31, 231–234, [https://doi.org/10.1130/0091-7613\(2003\)031<0231:EOMCMW>2.0.CO;2](https://doi.org/10.1130/0091-7613(2003)031<0231:EOMCMW>2.0.CO;2), 2003
 1744
 1745 Chappellaz, J., Blunier, T., Kints, S., Dällenbach, A., Barnola, J. M., Schwander, J., Raynaud,
 1746 D. and Stauffer B.: Changes in the atmospheric CH₄ gradient between Greenland and
 1747 Antarctica during the Holocene, *Geophys. Res. Lett.*, Volume 102, 15987-15997,
 1748 <https://doi.org/10.1029/97JD01017>, 1997
 1749
 1750 Cheng, A. L. and Huang, W. L.: Selective adsorption of hydrocarbon gases on clays and
 1751 organic matter, *Org. Geochem.*, 35, 413-423,
 1752 <https://doi.org/10.1016/j.orggeochem.2004.01.007>, 2004
 1753
 1754 Dan, J., Kumai, T., Sugimoto, A. and Murase, J.: Biotic and abiotic methane releases from
 1755 Lake Biwa sediment slurry, *Limnology* 5, 149–154, [https://doi.org/10.1007/s10201-004-](https://doi.org/10.1007/s10201-004-0124-7)
 1756 [0124-7](https://doi.org/10.1007/s10201-004-0124-7), 2004
 1757
 1758 Derendorp, L., Holzinger, R., Wishkerman, A., Keppler, F., and Röckmann, T.: VOC
 1759 emissions from dry leaf litter and their dependence on temperature, *Biogeosciences Discuss.*,
 1760 7, 823–854, <https://doi.org/10.5194/bgd-7-823-2010>, 2010
 1761
 1762 Derendorp, L., Holzinger, R., Wishkerman, A., Keppler, F., and Röckmann, T.: Methyl
 1763 chloride and C₂-C₅ hydrocarbon emissions from dry leaf litter and their dependence on
 1764 temperature, *Atmospheric Environment*, 45, 3112-3119,
 1765 <https://doi.org/10.1016/j.atmosenv.2011.03.016>, 2011
 1766
 1767 Dumelin, E.E. and Tappel, A.L.: Hydrocarbon gases produced during in vitro peroxidation of
 1768 polyunsaturated fatty acids and decomposition of preformed hydroperoxides, *Lipids*, 12, 894,
 1769 <https://doi.org/10.1007/BF02533308>, 1977
 1770
 1771 Dyonisius, M. N., Petrenko, V. V., Smith, A.M., Hua, Q., Yang, B., Schmitt, J., Beck, J.,
 1772 Seth, B., Bock, M., Hmiel, B., Vimont, I., Menking, J. A., Shackleton, S. A., Baggenstos, D.,
 1773

Feldfunktion geändert

1774 Bauska, T. K., Rhodes, R., Sperlich, P., Beaudette, R., Harth, C., Kalk, M., Brook, E. J.,
 1775 Fischer, H., Severinghaus, J. P. and Weiss, R. F.: Old carbon reservoirs were not important in
 1776 the deglacial methane budget, *Science*, 367(6480), 907-910,
 1777 <https://doi.org/10.1126/science.aax0504>, 2020
 1778
 1779 Erhardt, T., Bigler, M., Federer, U., Gfeller, G., Leuenberger, D., Stowasser, O.,
 1780 Röthlisberger, R., Schüpbach, S., Ruth, U., Twarloh, B., Wegner, A., Goto-Azuma, K.,
 1781 Kuramoto, T., Kjær, H. A., Vallenga, P. T., Siggaard-Andersen, M.-L., Hansson, M. E.,
 1782 Benton, A. K., Fleet, L. G., Mulvaney, R., Thomas, E. R., Abram, N., Stocker, T. F., and
 1783 Fischer, H.: High resolution aerosol concentration data from the Greenland NorthGRIP and
 1784 NEEM deep ice cores, *Earth Syst. Sci. Data Discuss.*, 14, 1215–1231,
 1785 <https://doi.org/10.5194/essd-14-1215>, 2022
 1786
 1787 Etiope, G. and Klusman, R. W.: Geologic emissions of methane to the atmosphere,
 1788 *Chemosphere*, 49, 8, 777-789, [https://doi.org/10.1016/S0045-6535\(02\)00380-6](https://doi.org/10.1016/S0045-6535(02)00380-6), 2002
 1789
 1790 Etiope G., Martinelli G., Caracausi, A. and Italiano, F.: Methane seeps and mud volcanoes in
 1791 Italy: gas origin, fractionation and emission to the atmosphere, *Geophys. Res. Lett.*, 34,
 1792 <https://doi.org/10.1029/2007GL030341>, 2007
 1793
 1794 Etiope G., Lassey K. R., Klusman R. W. and Boschi, E.: Reappraisal of the fossil methane
 1795 budget and related emission from geologic sources, *Geophys. Res. Lett.*, 35,
 1796 <https://doi.org/10.1029/2008GL033623>, 2008
 1797
 1798 Frahy, G. and Schopfer, P.: Hydrogen peroxide production by roots and its stimulation by
 1799 exogenous NADH, *Physiologia Plantarum*, 103, 395-404, <https://doi.org/10.1034/j.1399-3054.1998.1030313.x>, 1998
 1800
 1801 Flückiger J., Blunier T., Stauffer B., Chappellaz M., Spahni R., Kawamura K., Schwander J.,
 1802 Stocker T. F. and Dahl-Jensen D.: N₂O and CH₄ variations during the last glacial epoch:
 1803 Insight into global processes, *Global Biogeochem. Cy* 18, 1020,
 1804 <https://doi.org/10.1029/2003GB002122>, 2004
 1805
 1806 Fuhrer, K. and Legrand, M.: Continental biogenic species in the Greenland Ice Core Project
 1807 ice core: Tracing back the biomass history of the North American continent, *J. Geophys. Res.*,
 1808 102(C12), 26735– 26745, <https://doi.org/10.1029/97JC01299>, 1997
 1809
 1810 Georgiou, C. D., Sun, H. J., McKay, C. P., Grintzalis, K., Papapostolou, I., Zisimopoulos, D.,
 1811 Panagiotidis, K., Zhang, G., Koutsopoulou, E., Christidis, G. E. and Margiolaki, I.: Evidence
 1812 for photochemical production of reactive oxygen species in desert soils, *Nat.*
 1813 *Commun.*, 6, 7100, <https://doi.org/10.1038/ncomms8100>, 2015
 1814
 1815 Giorio, C., Kehrwald, N., Barbante, C., Kalberer, M., King, A. C. F., Thomas, E. R., Wolff,
 1816 E. W. and Zennaro, P.: Prospects for reconstructing paleoenvironmental conditions from
 1817 organic compounds in polar snow and ice, *Quaternary Science Reviews*, 183, 1-22,
 1818 <https://doi.org/10.1016/j.quascirev.2018.01.007>, 2018
 1819
 1820 Gu, Q., Chang, S. X., Wang, Z. P., Feng, J. C., Chen, Q. S. and Han, X. G.: Microbial versus
 1821 non-microbial methane releases from fresh soils at different temperatures, *Geoderma*, 284,
 1822 178-184, <https://doi.org/10.1016/j.geoderma.2016.08.027>, 2016
 1823
 1824

1825 Han, C., Do Hur, S., Han, Y., Lee, K., Hong, S., Erhard, T., Fischer, H., Svensson, A. M.,
 1826 Steffensen, J. P. and Vallelonga, P.: High-resolution isotopic evidence for a potential Saharan
 1827 provenance of Greenland glacial dust. *Sci Rep* 8, 15582, [https://doi.org/10.1038/s41598-018-](https://doi.org/10.1038/s41598-018-33859-0)
 1828 33859-0, 2018
 1829
 1830 Harris, E., Sinha, B., van Pinxteren, D., Tilgner, A., Wadinga Fomba, K., Schneider, J., Roth,
 1831 A., Gnauk, T., Fahlbusch, B., Mertes, S., Lee, T., Collett, J., Foley, S., Borrmann, S., Hoppe,
 1832 P. and Herrmann, H.: Enhanced Role of Transition Metal Ion Catalysis During In-Cloud
 1833 Oxidation of SO₂, *Science*, 340, 727–730, <https://doi.org/doi:10.1126/science.1230911>, 2013
 1834
 1835 Helmig, D., Petrenko, V., Martinerie, P., Witrant, E., Röckmann, T., Zuiderweg, A.,
 1836 Holzinger, R., Hueber, J., Thompson, C., White, J. W. C., Sturges, W., Baker, A., Blunier, T.,
 1837 Etheridge, D., Rubino, M., and Tans, P.: Reconstruction of Northern Hemisphere 1950–2010
 1838 atmospheric non-methane hydrocarbons, *Atmos. Chem. Phys.*, 14, 1463–1483,
 1839 <https://doi.org/10.5194/acp-14-1463>, 2014
 1840
 1841 Hoheisel, A., Yeman, C., Dinger, F., Eckhardt, H., and Schmidt, M.: An improved method for
 1842 mobile characterisation of $\delta^{13}\text{CH}_4$ source signatures and its application in Germany, *Atmos.*
 1843 *Meas. Tech.*, 12, 1123–1139, <https://doi.org/10.5194/amt-12-1123-2019>, 2019.
 1844
 1845 Hurkuck, M., Althoff, F., Jungkunst, H. F., Jugold, A. and Keppler, F.: Release of methane
 1846 from aerobic soil: An indication of a novel chemical natural process?, *Chemosphere*, 86, 684–
 1847 689, <https://doi.org/10.1016/j.chemosphere.2011.11.024>, 2012
 1848
 1849 Ji L., Zhang T., Milliken K. L., Qu J. and Zhang X.: Experimental investigation of main
 1850 controls to methane adsorption in clay-rich rocks, *Appl. Geochem.* 27, 2533–2545,
 1851 <https://doi.org/10.1016/j.apgeochem.2012.08.027>, 2012
 1852
 1853 John, W. W. and Curtis, R. W.: Isolation and Identification of the Precursor of Ethane
 1854 in *Phaseolus vulgaris* L., *Plant Physiology*, 59, 521–522, <https://doi.org/10.1104/pp.59.3.521>,
 1855 1977
 1856
 1857 Jugold, A., Althoff, F., Hurkuck, M., Greule, M., Lenhart, K., Lelieveld, J., and Keppler, F.:
 1858 Non-microbial methane formation in oxic soils, *Biogeosciences*, 9, 5291–5301,
 1859 <https://doi.org/10.5194/bg-9-5291-2012>, 2012
 1860
 1861 Katagi, T.: Photoinduced Oxidation of the organophosphorus Fungicide Tolclofs-methyl on
 1862 Clay Minerals, *J. Agric. Food Chem.*, 38, 1595–1600, 1990
 1863
 1864 Kaufmann, P. R., Federer, U., Hutterli, M. A., Bigler, M., Schüpbach, S., Ruth, U., Schmitt, J.
 1865 and Stocker, T. F.: An Improved Continuous Flow Analysis System for High-Resolution
 1866 Field Measurements on Ice Cores, *Environmental Science & Technology*, 42 (21), 8044–
 1867 8050, <https://doi.org/10.1021/es8007722>, 2008
 1868
 1869 Keeling, C. D.: The concentration and isotopic abundance of carbon dioxide in rural areas,
 1870 *Geochim. Cosmochim. Acta*, 13, 322–334 [https://doi.org/10.1016/0016-7037\(58\)90033-](https://doi.org/10.1016/0016-7037(58)90033-4)
 1871 4.1958, 1958
 1872
 1873 Keeling, C. D.: The concentration and isotopic abundance of carbon dioxide in rural and
 1874 marine air, *Geochim. Cosmochim. Acta*, 24, 277–298, [https://doi.org/10.1016/0016-](https://doi.org/10.1016/0016-7037(61)90023-0)
 1875 7037(61)90023-0, 1961

1876
1877 Keppler, F., Hamilton, J. T. G., Braß, M. and Röckmann, T.: Methane emissions from
1878 terrestrial plants under aerobic conditions, *Nature* 439, 187–191,
1879 <https://doi.org/10.1038/nature04420>, 2006
1880
1881 Keppler, F., Hamilton, J. T. G., McRoberts, W. C., Vigano, I., Braß, M. and Röckmann, T.:
1882 Methoxyl groups of plant pectin as a precursor of atmospheric methane: evidence from
1883 deuterium labelling studies, *New Phytologist*, 178, 808–814, [https://doi.org/10.1111/j.1469-](https://doi.org/10.1111/j.1469-8137.2008.02411.x)
1884 [8137.2008.02411.x](https://doi.org/10.1111/j.1469-8137.2008.02411.x), 2008
1885
1886 Kibanova, D., Trejo, M., Destaillets, H. and Cervini-Silva, J.: Photocatalytic activity of
1887 kaolinite, *Catalysis Communications*, 12, 698–702,
1888 <https://doi.org/10.1016/j.catcom.2010.10.029>, 2011
1889
1890 Köhler, P., Fischer, H., Schmitt, J., and Munhoven, G.: On the application and interpretation
1891 of Keeling plots in paleo climate research – deciphering $\delta^{13}\text{C}$ of atmospheric CO_2 measured in
1892 ice cores, *Biogeosciences*, 3, 539–556, <https://doi.org/10.5194/bg-3-539-2006>, 2006
1893
1894 Lee, L. E., Edwards, J. S., Schmitt, J., Fischer, H., Bock, M. and Brook, E. J.: Excess methane
1895 in Greenland ice cores associated with high dust concentrations, *Geochim. Cosmochim. Acta*,
1896 270, 409–430, <https://doi.org/10.1016/j.gca.2019.11.020>, 2020
1897
1898 Legrand, M., and Delmas, R.: Soluble Impurities in Four Antarctic Ice Cores Over the Last
1899 30000 Years, *Annals of Glaciology*, 10, 116–120,
1900 <https://doi.org/10.3189/S0260305500004274>, 1988
1901
1902 Liu, J., Chen, H., Zhu, Q., Shen, Y., Wang, X., Wang, M., Peng, C.: A novel pathway of
1903 direct methane production and emission by eukaryotes including plants, animals and fungi:
1904 An overview, *Atmospheric Environment*, 115, 26,
1905 <https://doi.org/10.1016/j.atmosenv.2015.05.019>, 2015
1906
1907 Liu, D., Yuan, P., Liu, H., Li, T., Tan, D., Yuan, W., He, H.: High-pressure adsorption of
1908 methane on montmorillonite, kaolinite and illite, *Applied Clay Science*, 85, 25–30,
1909 <https://doi.org/10.1016/j.clay.2013.09.009>, 2013
1910
1911 Lupker, M., Aciego, S. M., Bourdon, B., Schwander, J., and Stocker, T. F.: Isotopic tracing
1912 (Sr, Nd, U and Hf) of continental and marine aerosols in an 18th century section of the Dye-3
1913 ice core (Greenland), *Earth Pla Sci Let*, 295, 277–286,
1914 <https://doi.org/10.1016/j.epsl.2010.04.010>, 2010
1915
1916 McLeod, A. R., Newsham, K. K. and Fry, S.C.: Elevated UV-B radiation modifies the
1917 extractability of carbohydrates from leaf litter of *Quercus robur*, *Soil Biology and*
1918 *Biochemistry*, 39, Issue 1, 116–126, <https://doi.org/10.1016/j.soilbio.2006.06.019>, 2007
1919
1920 McLeod, A.R., Fry, S.C., Loake, G.J., Messenger, D.J., Reay, D.S., Smith, K.A. and Yun, B.-
1921 W.: Ultraviolet radiation drives methane emissions from terrestrial plant pectins, *New*
1922 *Phytologist*, 180, 124–132, <https://doi.org/10.1111/j.1469-8137.2008.02571.x>, 2008
1923
1924 Messenger, D.J., McLeod, A. R. and Fry, S.C.: The role of ultraviolet radiation,
1925 photosensitizers, reactive oxygen species and ester groups in mechanisms of methane

1926 formation from pectin, *Plant, Cell & Environment*, 32: 1-9, <https://doi.org/10.1111/j.1365->
1927 3040.2008.01892.x, 2009
1928
1929 Milkov, A. V. and Etiope, G.: Revised genetic diagrams for natural gases based on a global
1930 dataset of >20,000 samples, *Organic Geochemistry*, 125, 109-120,
1931 <https://doi.org/10.1016/j.orggeochem.2018.09.002>, 2018
1932
1933 Mitchell, L., Brook, E., Lee, J. E., Buizert, C., and Sowers, T.: Constraints on the Late
1934 Holocene anthropogenic contribution to the atmospheric methane budget, *Science* 342, 964–
1935 966, <https://doi.org/10.1126/science.1238920>, 2013
1936
1937 Miteva V., Teacher C., Sowers T. and Brenchley, J.: Comparison of the microbial diversity at
1938 different depths of the GISP2 Greenland ice core in relationship to deposition climates,
1939 *Environ. Microbiol.*, 11, 640–656, <https://doi.org/10.1111/j.1462-2920.2008.01835.x>, 2009
1940
1941 Möller, L., Sowers, T., Bock, M., Spahni, R., Behrens, M., Schmitt, J., Miller, H. and Fischer,
1942 H.: Independent variations of CH₄ emissions and isotopic composition over the past 160,000
1943 years, *Nature Geosci*, 6, 885–890, <https://doi.org/10.1038/ngeo1922>, 2013
1944
1945 Mohnen, D.: Pectin structure and biosynthesis, *Current Opinion in Plant Biology*, 11, 266–
1946 277, <https://doi.org/10.1016/j.pbi.2008.03.006>, 2008
1947
1948 NEEM community members: Eemian interglacial reconstructed from a Greenland folded ice
1949 core, *Nature*, 493, 489–494, <https://doi.org/10.1038/nature11789>, 2013
1950
1951 Nicewonger, M. R., Verhulst, K. R., Aydin, M. and Saltzman, E. S.: Preindustrial
1952 atmospheric ethane levels inferred from polar ice cores: A constraint on the geologic sources
1953 of atmospheric ethane and methane, *Geophys. Res. Lett.*, 43,
1954 <https://doi.org/10.1002/2015GL066854>, 2016
1955
1956 Nicewonger, M. R., Aydin, M., Prather, M. J., and Saltzman, E.S.: Large changes in biomass
1957 burning over the last millennium inferred from paleoatmospheric ethane in polar ice cores,
1958 *Proc. Natl. Acad. Sci. USA*, 115 (49), 12413-12418,
1959 <https://doi.org/10.1073/pnas.1807172115>, 2018
1960
1961 North Greenland Ice Core Project members, High-resolution record of Northern Hemisphere
1962 climate extending into the last interglacial period, *Nature* 431, 147–151,
1963 <https://doi.org/10.1038/nature02805>, 2004
1964
1965 Pires, J., Bestilleiro, M., Pinto, M. and Gil, A.: Selective adsorption of carbon dioxide,
1966 methane and ethane by porous clays heterostructures, *Separation and Purification*
1967 *Technology*, 61, 161-167, <https://doi.org/10.1016/j.seppur.2007.10.007>, 2008
1968
1969 Price, P. B. and Sowers, T.: Temperature dependence of metabolic rates for microbial growth,
1970 maintenance, and survival, *P. Natl. Acad. Sci. USA* 101, 4631–4636,
1971 <https://doi.org/10.1073/pnas.0400522101>, 2004
1972
1973 Rohde, R. A., Price, P. B., Bay, R. C. and Bramall, N. E.: In situ microbial metabolism as a
1974 cause of gas anomalies in ice, *P. Natl. Acad. Sci. USA*, 105, 8667–8672,
1975 <https://doi.org/10.1073/pnas.0803763105>, 2008
1976

1977 Rhodes, R. H., Faïn, X., Stowasser, C., Blunier, T., Chappellaz, C., McConnell, J. R.,
1978 Romanini, D., Mitchell, L. E. and Brook, E. J.: Continuous methane measurements from a
1979 late Holocene Greenland ice core: Atmospheric and in situ signals, *Earth and Planetary*
1980 *Science Letters*, 368, 9-19, <https://doi.org/10.1016/j.epsl.2013.02.034>, 2013
1981
1982 Rhodes, R. H., Faïn, X., Brook, E. J., McConnell, J. R., Maselli, O. J., Sigl, M., Edwards, J.,
1983 Buizert, C., Blunier, T., Chappellaz, J., and Freitag, J.: Local artifacts in ice core methane
1984 records caused by layered bubble trapping and in situ production: a multi-site investigation,
1985 *Clim. Past*, 12, 1061–1077, <https://doi.org/10.5194/cp-12-1061-2016>, 2016
1986
1987 Ross, D. J. K. and Bustin, R. M.: The importance of shale composition and pore structure
1988 upon gas storage potential of shale gas reservoirs, *Mar. Petrol. Geol.*, 26, 916-927,
1989 <https://doi.org/10.1016/j.marpetgeo.2008.06.004>, 2009
1990
1991 Ruth, U., Wagenbach, D., Steffensen, J. P. and Bigler, M.: Continuous record of microparticle
1992 concentration and size distribution in the central Greenland NGRIP ice core during the last
1993 glacial period, *J. Geophys. Res.*, 108 (D3), 4098, <https://doi.org/10.1029/2002JD002376>,
1994 2003
1995
1996 Ruth, U., Bigler, M., Röthlisberger, R., Siggaard-Andersen, M.-L., Kipfstuhl, S., Goto-
1997 Azuma, K., Hansson, M. E., Johnsen, S. J., Lu, H., and Steffensen, J. P.: Ice core evidence
1998 for a very tight link between North Atlantic and east Asian glacial climate, *Geophys. Res.*
1999 *Lett.*, 34, L03706, doi:10.1029/2006GL027876, 2007
2000
2001 Schade, G. W., Hofmann, R.-M. and Crutzen, P. J.: CO emissions from degrading plant
2002 matter, *Tellus B: Chemical and Physical Meteorology*, 51:5, 889-908,
2003 <https://doi.org/10.3402/tellusb.v51i5.16501>, 1999
2004
2005 Schilt, A., Baumgartner, M., Blunier, T., Schwander, J., Spahni, R., Fischer, H., and Stocker,
2006 T. F.: Glacial–interglacial and millennial-scale variations in the atmospheric nitrous oxide
2007 concentration during the last 800,000 years, *Quat Sci Rev*, 29, 182-192,
2008 <https://doi.org/10.1016/j.quascirev.2009.03.011>, 2010
2009
2010 Schmitt, J., Seth, B., Bock, M. and Fischer, H.: Online technique for isotope and mixing ratios
2011 of CH₄, N₂O, Xe and mixing ratios of organic trace gases on a single ice core sample, *Atmos.*
2012 *Meas. Tech.*, 7, 2645–2665, <https://doi.org/10.5194/amt-7-2645-2014>, 2014
2013
2014 Smith, H. J., Wahlen, M., Mastoianni, D., and Taylor, K. C.: The CO₂ concentration of air
2015 trapped in GISP2 ice from the Last Glacial Maximum-Holocene transition, *Geophys Res Lett*,
2016 24, 1-4, <https://doi.org/10.1029/96GL03700>, 1997
2017
2018 Sugimoto, A., Dan, J., Kumai, T. and Murase J.: Adsorption as a methane storage process in
2019 natural lake sediment, *Geophys. Res. Lett.* 30, 2080, <https://doi.org/10.1029/2003GL018162>,
2020 2003
2021
2022 Svensson, A., Biscaye, P. E. and Grousset, F. E.: Characterization of late glacial continental
2023 dust in the Greenland Ice Core Project ice core, *J. Geophys. Res.-Atmos.*, 105, 4637–4656,
2024 <https://doi.org/10.1029/1999JD901093>, 2000
2025

2026 Tian, Y., Yan, C. and Jin, Z.: Characterization of Methane Excess and Absolute Adsorption in
2027 Various Clay Nanopores from Molecular Simulation, *Sci Rep* 7, 12040,
2028 <https://doi.org/10.1038/s41598-017-12123>, 2017
2029
2030 Tung, H. C., Bramall, N. E. and Price, P. B.: Microbial origin of excess methane in glacial ice
2031 and implications for life on Mars, *P. Natl. Acad. Sci. USA* 102, 18292–18296,
2032 <https://doi.org/10.1073/pnas.0507601102>, 2005
2033 Tung, H., Price, P., Bramall, N. and Vrdoljak G.: Microorganisms metabolizing on clay
2034 grains in 3-km-deep Greenland basal ice, *Astrobiology* 6, 69–86.
2035 <https://doi.org/10.1089/ast.2006.6.69>, 2006
2036
2037 Vigano, I., van Weelden, H., Holzinger, R., Keppler, F., McLeod, A., and Röckmann, T.:
2038 Effect of UV radiation and temperature on the emission of methane from plant biomass and
2039 structural components, *Biogeosciences*, 5, 937–947, <https://doi.org/10.5194/bg-5-937-2008>,
2040 2008
2041
2042 Vigano, I., Röckmann, T., Holzinger, R., van Dijk, A., Keppler, F., Greule, M., Brand, W. A.,
2043 Geilmann, H. and van Weelden, H.: The stable isotope signature of methane emitted from
2044 plant material under UV irradiation, *Atmospheric Environment*, 43, 5637–5646,
2045 <https://doi.org/10.1016/j.atmosenv.2009.07.046>, 2009
2046
2047 Vigano, I., Holzinger, R., Keppler, F., Greule, M., Brand, W. A., Geilmann, H., van Weelden,
2048 H. and Röckmann, T.: Water drives the deuterium content of the methane emitted from plants,
2049 *Geochimica et Cosmochimica Acta*, 74, 3865–3873, <https://doi.org/10.1016/j.gca.2010.03.030>,
2050 2010
2051 Wang, Z.P., Han, X.G., Wang, G.G., Song, Y. and Gulledge, J.: Aerobic methane emission
2052 from plants in the Inner Mongolia steppe, *Environmental Science & Technology* 42, 62– 68
2053 <https://doi.org/10.1021/es071224l>, 2008
2054
2055 Wang, Z.P., Xie, Z.Q., Zhang, B.C., Hou, L.Y., Zhou, Y.H., Li, L.H. and Han, X.G.: Aerobic
2056 and Anaerobic Nonmicrobial Methane Emissions from Plant Material, *Environmental Science*
2057 *& Technology* 2011 45 (22), 9531–9537, <https://doi.org/10.1021/es2020132>, 2011
2058
2059 Wang, B., Hou, L., Liu, W. and Wang, Z.: Non-microbial methane emissions from soils,
2060 *Atmospheric Environment*, 80, 290–298, <https://doi.org/10.1016/j.atmosenv.2013.08.010>,
2061 2013
2062
2063 Wang, B., Lerdau, M. and He, Y.: Widespread production of nonmicrobial greenhouse gases
2064 in soils, *Glob Change Biol.*, 23:4472–4482, <https://doi.org/10.1111/gcb.13753>, 2017
2065
2066 Watanabe, M., Watanabe, Y., Kim, Y. S., Koike, T.: Dark aerobic methane emission
2067 associated to leaf factors of two Acacia and five Eucalyptus species, *Atmospheric*
2068 *Environment*, 54, 277–281, <https://doi.org/10.1016/j.atmosenv.2012.02.012>, 2012
2069
2070 Wehr, R. and Saleska, S. R.: The long-solved problem of the best-fit straight line: application
2071 to isotopic mixing lines, *Biogeosciences*, 14, 17–29, <https://doi.org/10.5194/bg-14-17-2017>,
2072 2017.
2073
2074 Whiticar, M. J.: Carbon and hydrogen isotope systematics of bacterial formation and
2075 oxidation of methane, *Chemical Geology*, 161, 291–314, [https://doi.org/10.1016/S0009-](https://doi.org/10.1016/S0009-2541(99)00092-3)
2076 [2541\(99\)00092-3](https://doi.org/10.1016/S0009-2541(99)00092-3), 1999

2077
2078 Wu, F., Li, J., Peng, Z., Deng, N.: Photochemical formation of hydroxyl radicals catalyzed by
2079 montmorillonite, *Chemosphere*, 72, 407-413,
2080 <https://doi.org/10.1016/j.chemosphere.2008.02.034>, 2008
2081
2082 York, D.: Least squares fitting of a straight line with correlated errors, *Earth and Planetary*
2083 *Science Letters*, 5, 320-324, [https://doi.org/10.1016/S0012-821X\(68\)80059-7](https://doi.org/10.1016/S0012-821X(68)80059-7), 1968
2084
2085 York, D., Evensen, N. M., Martinez, M. L., and De Basabe Delgado, J.: Unified equations for
2086 the slope, intercept, and standard errors of the best straight line, *Am. J. Phys.* 72, 367-375,
2087 <https://doi.org/10.1119/1.1632486>, 2004